ROCK DIFFERENTIATION USING MICROWAVE IRRADIATION

Sean R. Mercer

BSc(Eng) Cape Town

Thesis submitted to the Department of Electrical and Electronic Engineering of the University of Cape Town in fulfilment of the requirements for the Degree MSc(Eng).

DECLARATION

I declare that this dissertation is my own unaided work. It is being submitted in fulfilment of the requirements for the degree of Master of Science in Engineering at the University of Cape Town. It has not been submitted before for any degree or examination at any other university.

Signed by candidate

(Signature of Candidate)

30th day of September 1987

ABSTRACT

This project arose as a result of inefficiencies in the diamond recovery process at Premier Mine. A considerable amount of barren waste rock, gabbro, is mined along with the diamond bearing kimberlite. No automated method exists for separating the kimberlite from the waste rock and a device was required to effect ore sorting on a rock by rock basis.

Experimentation with a microwave oven indicated that samples of kimberlite were more attenuative than samples of gabbro. The possibility of using microwave heating for rock differentiation was investigated but was shown to be impractical to implement.

A study of low power microwave attenuation and reflection measurements was undertaken. Reflection measurements were found to be impractical due to the similar amounts of reflected signal from the different rock types. Microwave signal attenuation through rock samples was studied over a broad frequency spectrum. A detectable difference in signal attenuation was found through the gabbro and kimberlite. The difference in signal attenuation increased with increasing frequency.

Different techniques to implement signal attenuation measurements through rock samples were investigated. The passing of rock samples through waveguide structures was found to be impractical in this application. Microwave signal attenuation measurements were successful when rock samples were placed between a transmitting and a receiving antenna.

Equipment was designed and constructed with an operating frequency of 35GHz chosen due to the small antenna aperture area and the large attenuation difference at this frequency. Static measurements with this equipment revealed the problems

with signal scattering and reflection from some irregularly shaped samples of low loss gabbro. The importance of these phenomenon could only be gauged from dynamic measurements.

Dynamic measurements were performed using a laboratory test system with a conveyor belt capable of moving at speeds of up to 5 m/s. It was found that 93% of the kimberlite could be correctly detected whilst rejecting 67% of the gabbro. The system functioned satisfactorily and led to the filing of several patents.

ACKNOWLEDGEMENTS

The author wishes to thank Professor B.J. Downing for his guidance and support during this project.

The author would like to thank De Beers Diamond Research Laboratories for their financial support,assistance and co-operation in supplying rock samples for this project. In particular, thanks are due to Dr. D. Salter and other De Beers personnel, including Mr L. Nordin, for their technical assistance and advice.

The financial assistance from the Council for Scientific and Industrial Research was gratefully appreciated.

CONTENTS

LIST OF FIGURES

1. INTRODUCTION

Premier Mine at Cullinan,South Africa, is the site of the third largest diamond pipe in the Southern Hemisphere [1]. The Premier pipe is a complex multiple intrusion which consists of a variety of diamond bearing kimberlitic rocks. The kimberlite pipe has been intruded by a sill of non diamond bearing gabbro as shown in figure 1.1.

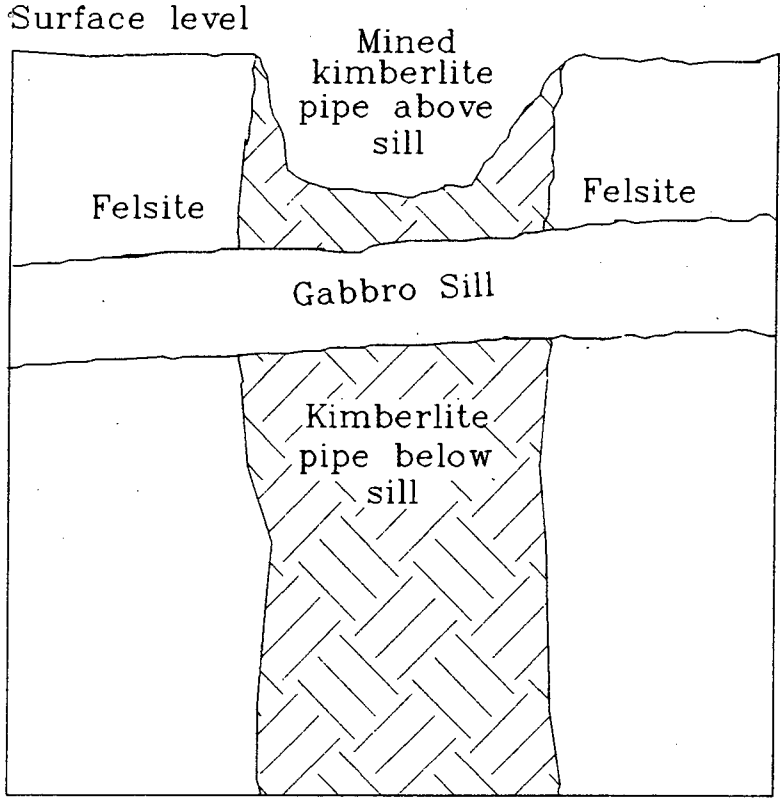

Fig.1.1 Simplified diagram of Premier kimberlite pipe.

When mining began at Premier in 1902, open cast mining techniques were used. Conventional sub level or open bench mining techniques remained in use until the discovery of the gabbro sill approximately 400m below the surface. The gabbro sill is some 75m thick and consists of approximately 52

million tons of rock within the confines of the pipe. The gabbro cannot be mined economically due to it's volume and the high cost of removing it.

The presence of the gabbro sill has posed many problems to the Premier mining engineers. The most significant of these is the admixing of the barren gabbro with the kimberlite below the sill due to the poor geotechnical properties of the sill. Large volumes of gabbro continually drop onto the mining areas causing large scale dilution of the kimberlite. This problem is gradually being brought under control but will be a feature of the mine for many years to come. There are currently only 3 years of kimberlite ore reserves remaining above the sill. All future production must therefore come from below the sill mining areas.

At present,ore is being drawn from both above and below the sill. However,as noted above,the limited life of above-sill workings means that the gabbro problem is soon to become proportionately more serious. The problem manifests itself in the following ways:

1. Gabbro replaces valuable kimberlite in the treatment plant's headfeed and therefore reduces its potential revenue generating capability.

2. Gabbro is subjected to the full diamond liberation and recovery process - clearly a wasteful and expensive exercise.

3. Gabbro follows the diamond route through the treatment plant. However,since this process route is designed to concentrate diamond into a very low mass,low volume,high value stream it is consequently overloaded when large volumes of gabbro accompany the diamond product. This leads to tremendous operational difficulties.

A means of separating the gabbro from the kimberlite was therefore required: an automatic sorting technique capable of differentiating between kimberlite and gabbro on a rock by rock basis being the ultimate goal. Further,since the rocks are of a non-uniform shape and size,and for practical reasons in the treatment of large volumes of rock,a non-contact discrimination technique was required. No existing commercial technology was found to be able to differentiate between gabbro and kimberlite.

Preliminary experiments were performed by De Beers personnel using similar sized samples of gabbro and kimberlite. These were irradiated with microwave energy in a microwave oven. It was found that the kimberlite became hotter than the gabbro when the samples were irradiated for equal periods of time.

This indicated that the kimberlite had absorbed or attenuated the microwave signal more than the gabbro. For this reason it was decided to consider the possibility of using microwave irradiation to distinguish between samples of gabbro and kimberlite.

The objective of this project was to develop and construct a suitable device to differentiate between kimberlite and gabbro.

2. CONCEPT STATEMENT

2.1 Relevant theory

Consideration is given to the propagation of an electromagnetic wave through a conducting linear, isotropic and homogeneous medium. For a sinusoidal, time dependent electromagnetic wave polarised in the **x** axis direction and travelling through a conducting linear, isotropic and homogeneous medium, the solution to the Wave Equation is:

$$E_x = E_p e^{jwt \pm \Lambda x}$$

where E_x = **x** axis component of the electric field

E_p = Peak value of the electric field

w = angular frequency of the wave in radians

$\Lambda = jw\sqrt{\mu\epsilon(1+\sigma/jw\epsilon)}$

= Propagation constant for the medium

where $\mu = \mu_o\mu_r$ = Absolute permeability of the medium

$\epsilon = \epsilon_o\epsilon_r$ = Absolute permittivity of the medium

and σ = Conductivity of the medium

The Propagation constant can be expressed as:

$$\Lambda = \alpha + j\beta \qquad .....(2.2)$$

where α = Attenuation constant in dB/m

β = Phase constant in radians

Substituting equation (2.2) into equation (2.1) we obtain

$$E_x = E_p e^{-\alpha x} e^{j(wt \pm \beta x)} \qquad .....(2.3)$$

It can be seen from equation (2.3) that when propagating through a medium with a non zero attenuation constant α, an electromagnetic wave will experience an exponential decay through the medium. The rate of decay through the medium will depend on α for the medium.

The propagation constant for a medium can be expressed as:

$$\gamma = \sqrt{\mu\sigma w/2} + j\sqrt{\mu\sigma w/2} \qquad .....(2.4)$$

From equation (2.4) it can be seen that α is directly proportional to the square root of the frequency of the incident signal, provided that μ and σ do not vary. This means that as the incident signal frequency is increased, the signal attenuation through a conducting medium will increase.

It is shown in the literature [2] that the attenuation constant α for a conducting medium can be expressed as:

$$\alpha = w/c\sqrt{\epsilon_r/2}[\sqrt{1+(\sigma/w\epsilon_o\epsilon_r)^2}-1]^{\frac{1}{2}} \qquad .....(2.5)$$

where ϵ_r = dielectric constant for the medium
c = propagation velocity of the electromagnetic wave in the medium

Equation (2.5) indicates that the attenuation constant α for a medium will be dependent on the dielectric constant of the medium. If two different media have different dielectric constants then their attenuation constants will differ and the two media will exhibit different amounts of signal attenuation. It can also be seen from equations (2.4) and (2.5) that two media with different conductivities, σ, will exhibit different amounts of signal attenuation even if they have the same value of ϵ_r.

2.2 Discussion

All rock types are composed of an aggregate of minerals of a certain composition and in a certain proportion to one another. All rock types also contain a certain inherent volume of water, bound up in the form of waters crystallisation, pore water or surface water. Due to their

varied composition, all minerals and rock types will have a finite range of dielectric constants.

The structure of a rock can also influence its electrical properties. Preferential orientation of certain minerals in a rock can lead to anisotropy of its electrical properties [3]. The complex structure of kimberlite with its many randomly arranged component minerals may well exhibit anisotropy of its dielectric constant. This factor may have to be considered when attenuation measurements are performed on rock samples.

In the light of results of the heating tests performed on samples of gabbro and kimberlite by De Beers personnel, a study of rock heating was undertaken. The possibility of using microwave transmission or reflection measurements for rock differentiation was also considered.When transmission measurements are considered, the measurement of signal attenuation and/or phase shift can be examined.

A survey of the literature [4-7] revealed the use of both signal attenuation and phase shift in determining the moisture content of a bulk material. The development time of a device to accurately measure microwave signal phase shift is long and is relatively expensive due to its inherent complexity. The development time of a microwave signal attenuation meter is far shorter due to its relative simplicity. The use of microwave attenuation measurements has been successfully employed to monitor the moisture content of a bulk material [8].

As noted in section 1,the problem of sorting waste gabbro from kimberlite is one that exists at present and requires a solution as soon as possible . It is for the above reasons that consideration was give to a device using microwave attenuation measurements rather than phase shift measurements. A study of signal phase shift measurements can be performed at

a later date should this prove necessary.

3. ROCK IRRADIATION USING A MICROWAVE OVEN

Preliminary heating experiments had been performed on samples of gabbro and kimberlite by De Beers personnel. It was decided to repeat these heating experiments to confirm the initial test results. The effect of ore moisture content on the temperature difference between gabbro and kimberlite was investigated as this parameter is variable in the processing of ore.

Roughly shaped ore samples with an approximate mass of 300g were examined. The temperature decay of the heated rocks was recorded using a Chromel P/Alumel thermocouple. Holes were drilled into the rock samples so that the thermocouple could be inserted into the rock to measure the temperature. This was found to be more accurate than recording the surface temperature of a rock using a thermometer.

The thermocouple was connected directly to a millivolt meter. Although more accurate results could have been obtained using a reference junction this was not considered necessary as the temperature difference between gabbro and kimberlite, rather than the absolute temperature, was important here. The thermocouple output voltage increases with increasing temperature.

3.1 Experimental results and discussion

Dry samples of gabbro and kimberlite were irradiated in a 2.45GHz, 500W microwave oven for one minute each. The respective cooling rates for these samples are shown in figure 3.1. The same rock samples were then completely immersed in water for up to 48 hours. These were then irradiated in the microwave oven for one minute each. The cooling rates for these wet rocks are also shown in figure 3.1.

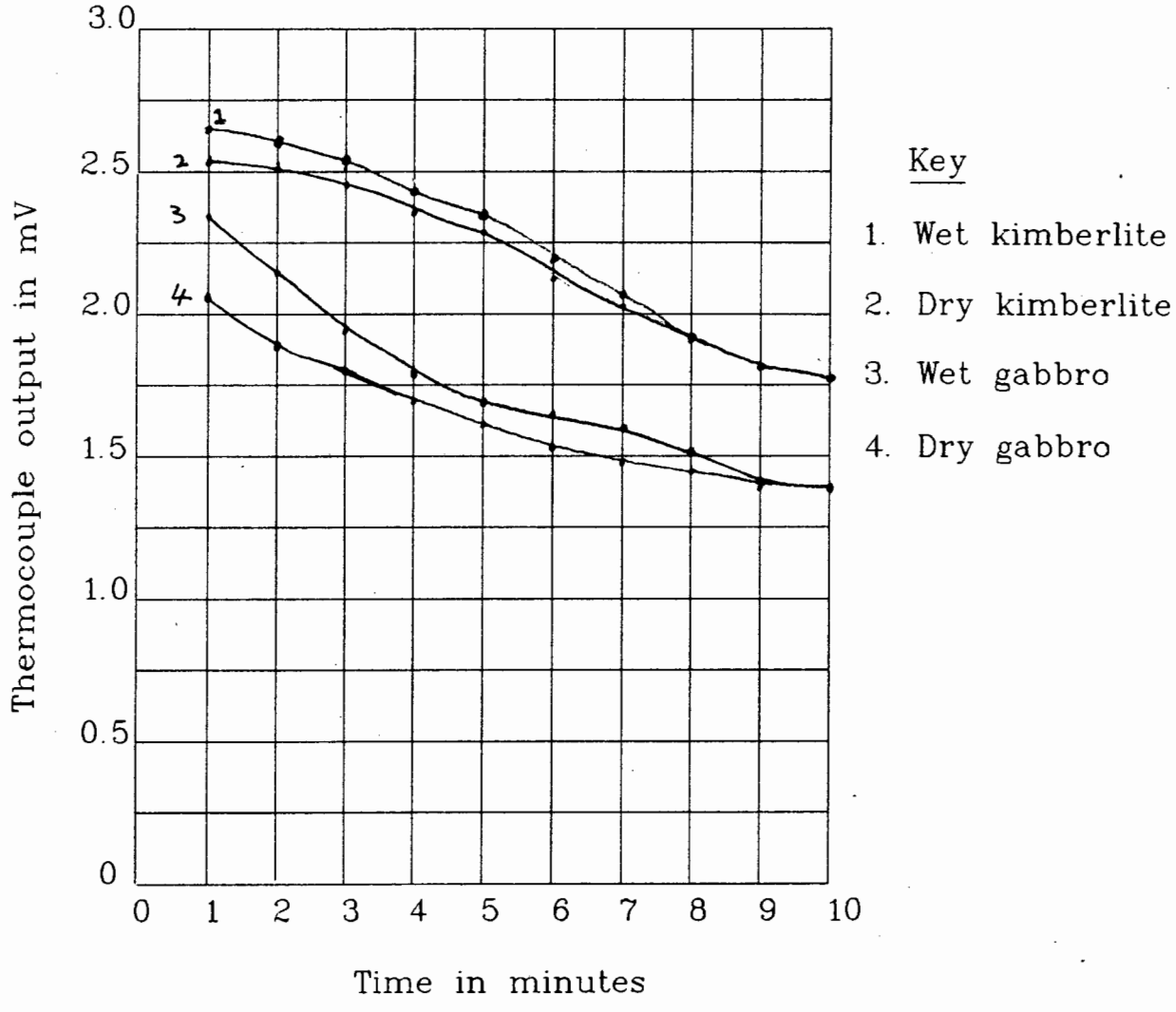

Fig 3.1 Thermocouple output for wet and dry gabbro and kimberlite.

The curves for dry gabbro and dry kimberlite indicate that the kimberlite was initially hotter than the gabbro and remained hotter as the rocks cooled down. This situation also occurred for the wet gabbro and the wet kimberlite. The curves in figure 3.1 indicate that the initial temperature difference between gabbro and kimberlite was reduced when the rock samples were wet. The initial temperature of the wet gabbro had increased more than the initial temperature of the wet kimberlite.

Rock differentiation on the basis of the level of microwave signal attenuation would be most reliable at a frequency where the difference in attenuation between rock types is greatest. For this reason, microwave frequencies with resonant moisture absorption peaks such as 23GHz should be avoided.

In practice the rocks will be wet when they are to be separated because they are washed prior to the treatment processes. It is more difficult to reliably detect a small temperature difference than a large temperature difference. The initial temperature difference must be considered since no time delay can be implemented in existing sorting machines employing conveyor belt speeds of 5m/s.

The literature advocates the use of an infrared camera system to record the surface temperature of ore samples but this is known to be inaccurate [9]. These factors tend to indicate that the heating of wet rock samples and the reliable detection of a temperature difference would not be a practical system to implement.

The cost effectiveness of an on line rock heating plant must also be considered. The literature describes the dielectric heating of small laboratory size ore samples [9,10]. The calculation given in Appendix A, however, indicates that the power requirements to heat the necessary tonnage of rock is excessively high and is impractical to implement.

4. LOW POWER MICROWAVE SIGNAL INVESTIGATION

The microwave rock heating tests at 2.45GHz using a microwave oven indicated that there was a difference in signal attenuation or reflection between similar sized samples of gabbro and kimberlite at that frequency. The use of a high powered microwave heating plant for rock differentiation was, however, deemed impractical due to the very high power required. The possibility of using low power microwave signal measurements for rock differentiation was therefore considered.

An investigation of microwave signal reflection and insertion loss due to the presence of rock samples was undertaken with a view to devising a device for rock identification on a rock by rock basis. A broad frequency spectrum was examined to determine if a particular microwave frequency displayed a marked difference in signal attenuation between the different rock types.

Two different techniques were used to investigate the microwave signal attenuation or insertion loss through the different rock types. One method was to investigate the signal transmission between two antennae. A different approach was to investigate the passing of a rock through a waveguide structure on signal transmission through the waveguide.

4.1 Investigation of microwave signal attenuation using propagation between two antennae

A Hewlett Packard 8350B sweep oscillator was used for this investigation. This device is capable of generating signals in the frequency range 10MHz to 26.5 GHz. A Hewlett Packard 8410C network analyser, linked to a Hewlett Packard 8746B S-

parameter test set, was coupled to the sweep oscillator. This equipment was interfaced to an HP 85 microcomputer via an HP59313A A/D convertor.

The above equipment was set to measure the S-parameter S_{21} over a frequency range from 9GHz to 16.4GHz. This allowed measurements of the insertion loss or attenuation through the rock samples to be measured. High frequency coaxial cables were connected to the S-parameter test set ports. Square waveguide antennae were connected to the coaxial cables by means of coaxial cable to rectangular waveguide and rectangular to square waveguide transformers as shown in figure 4.1. An open square waveguide operates as an efficient, well matched, low cost antenna which is physically small.

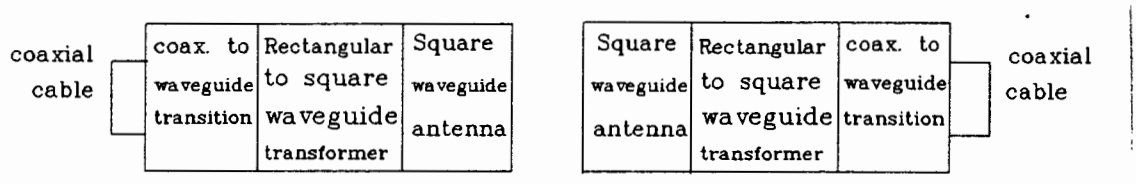

Fig.4.1 Connection of antennae.

The antennae were mounted on a rigid test frame and aimed at each other. Measurements of the insertion loss due to rock samples between the antennae could be obtained using this configuration. The HP85 microcomputer was used to calibrate the system to compensate for path loss between the antennae and possible losses due to any impedance mismatching in the system.

Reliable measurements of S_{21} were not possible above 16.4 GHz due to the frequency limitations of the network analyser. This meant that a different technique of data acquisition was required for testing at frequencies above 16.4GHz. At these

frequencies one of the antennae indicated in figure 4.1 was coupled directly to the output of the sweep oscillator by means of a coaxial line. A Hewlett Packard 8485A power sensor was connected to the coaxial cable output of the second antenna unit. The power sensor was connected to a HP435A power meter.

The antennae were mounted facing each other in the test frame as before. The insertion loss due to a rock sample placed between the antenna could then be determined by first measuring the received power in dBm with no rock between the antennae. The rock would then be placed between the antennae and the received power in dBm would be noted again. The insertion loss due to the rock sample in dB was obtained by calculating the difference between these two readings.

In order to irradiate rock samples with a broad frequency spectrum of microwave signals a range of different antennae had to be designed and constructed for operation at different frequencies. Rectangular to square waveguide transformers also had to be designed and fabricated. The test frame also had to be designed and fabricated to maintain antenna alignment whilst data were acquired.

4.1.1 Design of square waveguide antennae and rectangular to square waveguide transformers.

Square waveguide antennae were chosen for simplicity and the fact that they provide a reasonable impedance match to air. Antennae were designed for S band, X band, J band and K band frequencies to propagate over the required frequency range. This meant that rectangular to square waveguide transformers had to be designed to couple these antennae to rectangular waveguide sections.

Consider the design of the X band rectangular to square

waveguide transformers:
For a rectangular waveguide

$$\lambda_g = \frac{\lambda}{\sqrt{1-\left(\frac{\lambda}{2a}\right)^2}}$$

where a is the width of the broad wall of the rectangular waveguide in cm,

λ = freespace wavelength in cm
λ_g = waveguide wavelength in cm

Using f= 10 GHz (approximate centre frequency of X band)
λ = c/f = 3cm

For X band waveguide, a = 2.286 cm
and λ_g = 3.976 cm

A $\lambda/4$ long rectangular to square waveguide transformer is shown in figure 4.2.

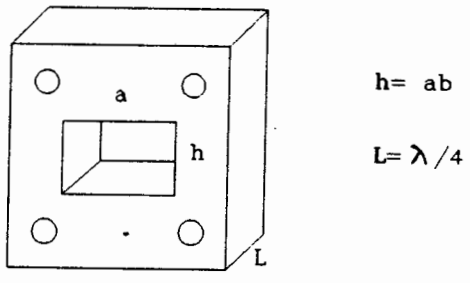

Fig.4.2 Rectangular to square waveguide transformer.

Rectangular waveguide has internal dimensions a*b where a is the longest side and b is the lesser dimension. The height of the slot in the rectangular to square waveguide transformer is given by the relation

h = a*b

For X band waveguide a = 2.286 cm and b = 1.016 cm
so h = 1.524 cm.

This procedure was used to design the rectangular to square waveguide transformers listed in figure 4.3.

	L	a	b	h
S band	13.898cm	7.200cm	3.400cm	4.945cm
X band	0.994cm	2.286cm	1.016cm	1.52cm
J band	0.632cm	1.579cm	0,789cm	1.12cm
K band	0.435cm	1.067cm	0.432cm	0.68cm

Fig. 4.3 Rectangular to square waveguide transformer dimensions.

The complete design criteria for these matching sections are included in Appendix B.

The internal dimensions of a square waveguide antenna are a*a where a is the dimension of the longest side of the rectangular waveguide to which it is to be coupled. The lengths of these antennae were not critical and were chosen for convenient manufacture. The square waveguide antenna dimensions are given in figure 4.4

	a in cm	Antenna length
S band	7.200 cm	10.0 cm
X band	2.286 cm	5.0 cm
J band	1.579 cm	5.0 cm
K band	1.067 cm	5.0 cm

Fig 4.4 Antenna dimensions.

The complete design criteria for these antennae are included in Appendix B.

4.1.2 Design of test frame and coaxial to waveguide transformer.

Coaxial cable to rectangular waveguide transformers had to be designed for S band where manufactured units were not readily available. The construction of a 3GHz coaxial cable to rectangular waveguide transformer was undertaken using a commercial unit as a template.

A wooden test frame was designed and fabricated to hold and accurately align the antennae, thereby minimising impedance mismatching. The rigid structure of the test frame reduced the possibility of errors occurring due to changing path length or lateral antennae movement. The construction of the frame was such that one antenna could be moved whilst remaining aligned with the fixed antenna.

This structure allowed the antennae to be placed as close to the rock samples as possible to minimise path loss and

signal refraction around the samples. The test frame is illustrated in figure 4.5.

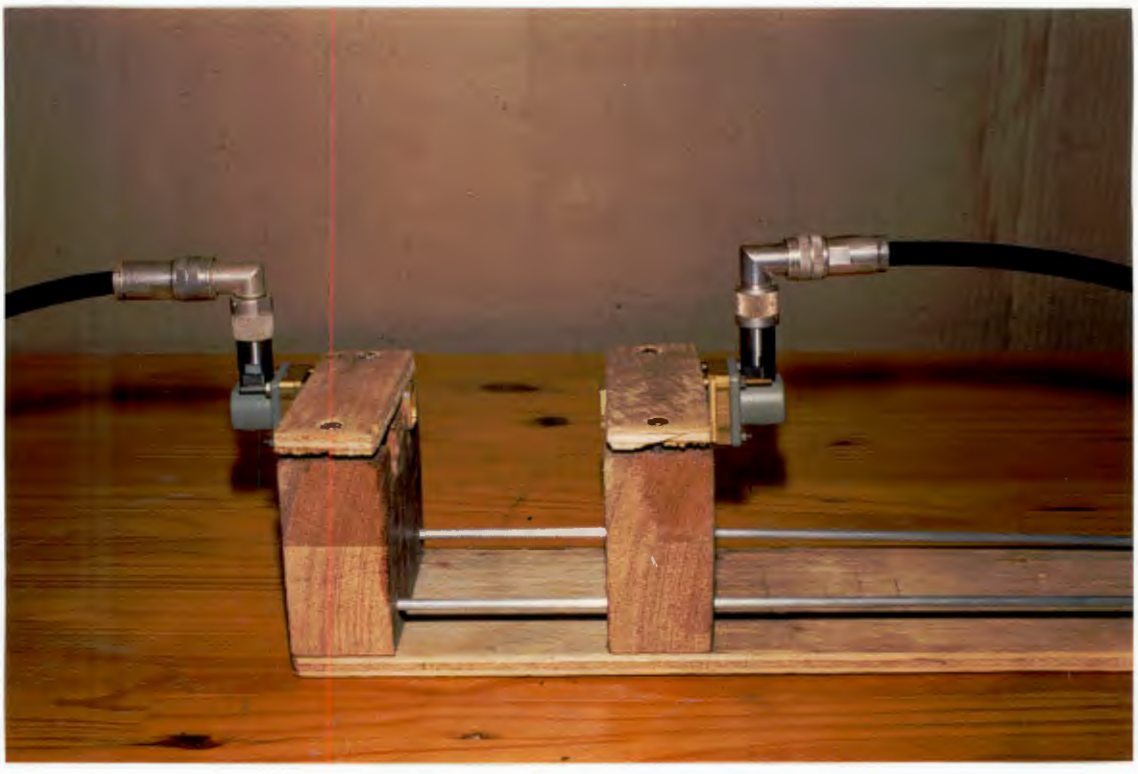

Fig.4.5 The test frame.

4.1.3 Experimental procedure

The microwave signal attenuation due to ore samples of varied geometry was investigated. Smooth surfaced, parallel sided rock samples of different thicknesses were cut for examination. Accurate signal attenuation measurements were only possible when the entire antenna aperture area was covered by a rock sample. Microwave signal reflections from rock samples and signal creepage around rock samples can adversely affect the measured values of signal attenuation. The use of suitably sized, parallel sided rock samples should minimise these effects. Rocks of different thicknesses and random shapes were also examined.

For signal frequencies between 3GHz and 16.4GHz the correct antennae were mounted on the test frame and spaced close to the rock to minimise signal creepage around the rock. The antennae were coupled to the S-parameter test set and the system was calibrated using the HP85 microcomputer. Rock samples were then inserted between the antennae and measurements of insertion loss due to the rock were obtained. These readings were repeated using many different rock samples and the resultant curves were plotted.

The system was also calibrated with a slab of gabbro between the antennae. The insertion loss of kimberlite samples were then measured relative to this calibration curve. This technique provided a clear indication of the attenuation difference between these rock types at different frequencies.

For signal frequencies ranging from 16.4GHz to 26.5GHz the appropriate antennae were connected to the sweep oscillator and power meter as described in section 4.1. Repeated measurements were obtained using different rock samples. A study of microwave signal attenuation through separated component minerals of kimberlite was also undertaken. The effect of moisture content on the insertion loss due to rock samples was also studied.

4.1.4 Results

A selection of the results of the microwave signal attenuation tests are included in the ensuing text.

The S band antennae coupled to the network analyser were used to examine insertion loss over the frequency range from 2.6GHz to 3.9GHz. A detectable difference in signal

attenuation between samples of kimberlite and samples of gabbro and felsite was observed. The average attenuation figures due to these rock types at a frequency of 3GHz are given in figure 4.6.

Rock type	Average attenuation in dB/cm
Kimberlite	2.01 dB/cm
Gabbro	0.44 dB/cm
Felsite	0.33 dB/cm

Fig 4.6 Average attenuation at 3GHz.

The X band antennae were used to obtain the curves for parallel sided 2cm thick samples of gabbro and kimberlite that are shown in figure 4.7. Similar trends were observed with other 2cm slabs of gabbro and kimberlite.

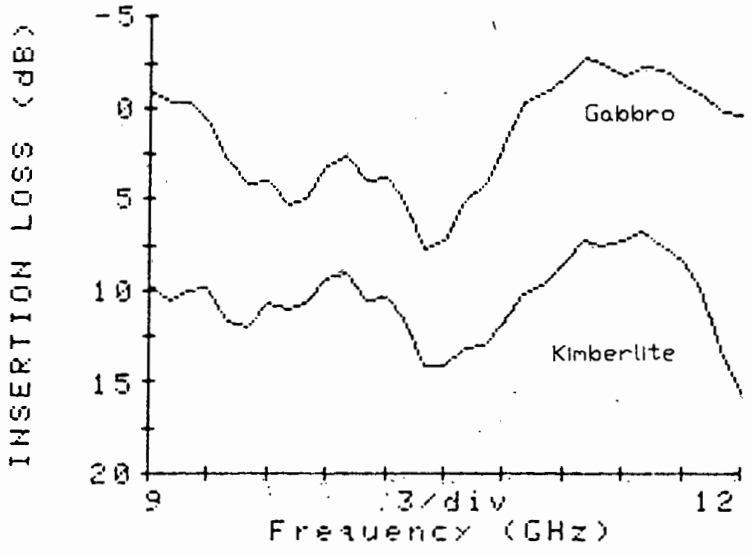

Fig.4.7 X band insertion loss for 2cm thick rocks.

The same rock samples were used for the J band curves of insertion loss illustrated in figure 4.8. The curves of figure 4.7 and figure 4.8 do not join at 12 GHz due to the use of different waveguide antennae and consequently different antenna gains. The results obtained at the extreme operating frequencies of the antennae may be inaccurate due to possible antenna impedance mismatching and antenna gain variation with frequency.

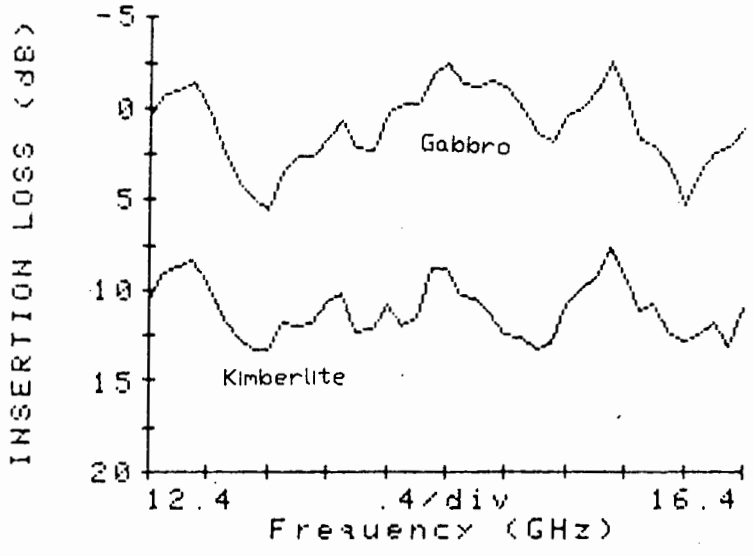

Fig.4.8 J band insertion loss for 2cm thick rocks.

When the system was calibrated with a sample of gabbro between the antennae a clear indication of the difference in attenuation between kimberlite and other rock types was obtained. The curves of figure 4.9 and figure 4.10 indicate the difference in signal attenuation between 2cm thick samples of gabbro and kimberlite at X band and J band.

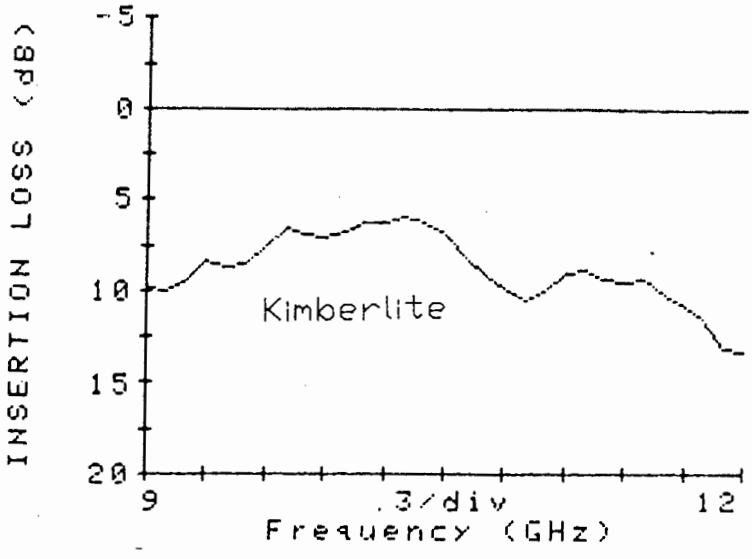

Fig.4.9 Difference in insertion loss between gabbro and kimberlite at X band.

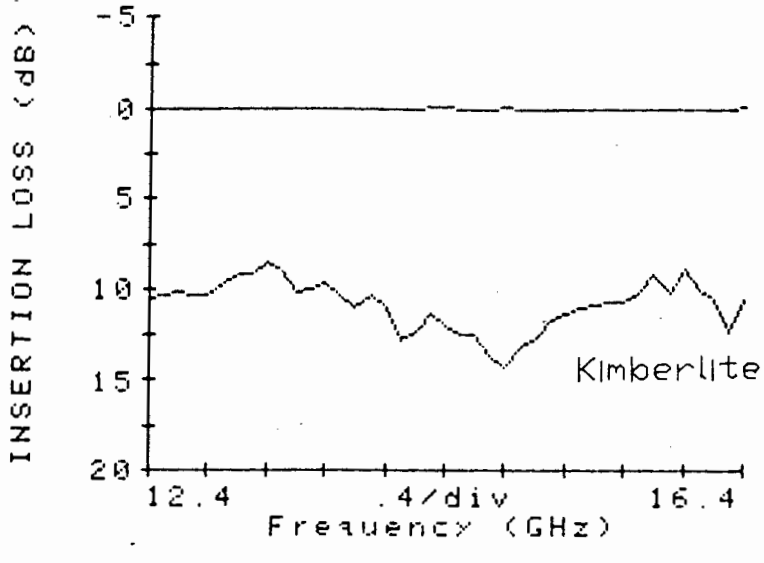

Fig.4.10 Difference in insertion loss between gabbro and kimberlite at J band.

A study of the average signal attenuation due to the various rock types was performed at 10GHz. These results are shown in figure 4.11.

Rock type	Average attenuation in dB/cm
Kimberlite	2.17 dB/cm
Gabbro	0.49 dB/cm
Felsite	0.56 dB/cm

Fig.4.11 Average attenuation at 10GHz.

The effect of moisture on insertion loss was also examined. Samples of gabbro and kimberlite were measured when dry and after being immersed in water for 24 hours. It was found that moisture content had little effect on the insertion loss, probably due to the small amount of water absorbed by the rocks. The effect of moisture was most noticeable at frequencies around 23GHz due to the existence of a moisture absorbtion peak at 23GHz. At this frequency the difference in insertion loss between gabbro and kimberlite was reduced by 1.7dB. The effect of moisture content on insertion loss was therefore considered negligible in this application, provided that frequencies with resonant moisture absorption peaks were avoided.

The sweep oscillator and power meter were then used to obtain data for frequencies above 16.4GHz. The average values of signal attenuation for gabbro, kimberlite and felsite, in dB/cm, are shown in figure 4.12.

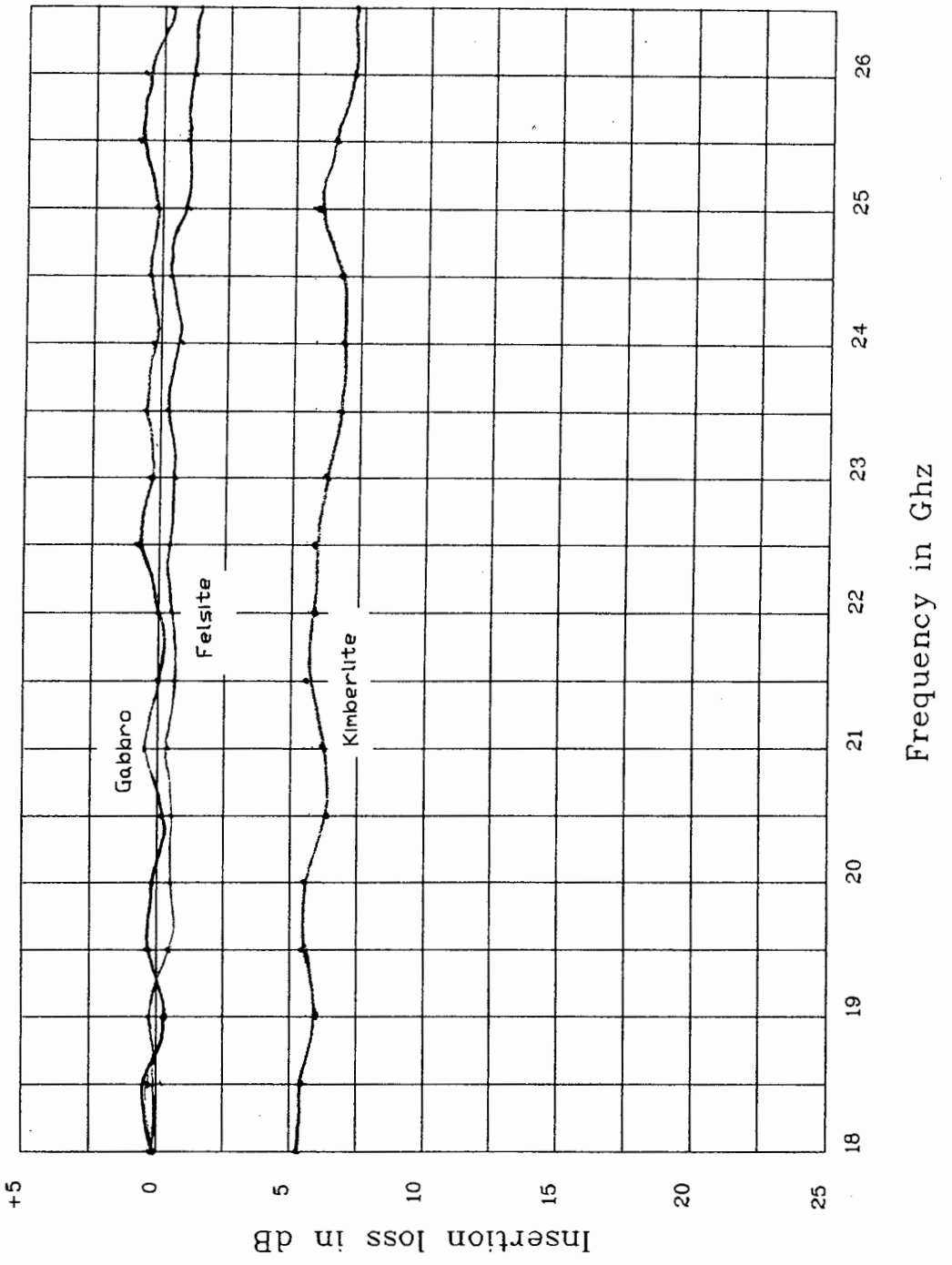

Fig.4.12 Insertion loss at K band.

A further study of signal attenuation through kimberlite was performed at different frequencies. It was found that grey kimberlite and piebald kimberlite,two common Premier kimberlite types, had virtually identical attenuation characteristics at microwave frequencies. Kimberlite is composed of many different component minerals and is a generic name for a great variety of

rocks. A study of signal attenuation using component minerals that had been separated from kimberlite was undertaken using different frequencies. The expected trend of increasing attenuation with increasing signal frequency was observed using these minerals. The average signal attenuation through some of these minerals is shown in figure 4.13.

Kimberlite component	Average attenuation
Chrome Diopside	1.55 dB/cm
Garnet	3.1 dB/cm
Ilmenite	8.47 dB/cm
tailings	5.35 dB/cm

Fig.4.13 Average attenuation through kimberlite component minerals at X band.

These results indicate that the 'kimberlite' has component minerals with widely varying attenuative properties. These component minerals are present in different proportions in different samples of kimberlite. Despite its structure, however, the various results indicate that consistent attenuation values were obtained with kimberlite samples.

Randomly shaped rock samples were also studied. Similar trends of increasing attenuation with increasing frequency were observed. This form of measurement was more difficult to perform accurately because of the geometry of the samples. It had to be ensured that no signal could pass directly between the antennae.

When examining figures 4.7, 4.8, 4.9, 4.10 and 4.12 it

can be seen that no single frequency displays a sudden increase in attenuation through kimberlite and not through gabbro or felsite. It can be seen from figures 4.6 and 4.11 that the difference in attenuation between gabbro and kimberlite increases with increasing frequency. The overall signal attenuation through the rock types also increased with increasing frequency.

This would tend to indicate that the equipment used to differentiate between different rock types should operate at the highest possible operating frequency to obtain the largest difference in signal attenuation between the two rock types. The antenna dimensions of figure 4.4 indicate that the antenna aperture area decreases with increasing frequency. This also points to the use of a high operating frequency since the smaller the antenna aperture area then the smaller the rock samples for differentiation can be.

4.2 Examination of signal attenuation in waveguide structures

One technique of irradiating rock samples with microwave signals was to pass rocks between a transmit and a receive antenna and note the received signal amplitude variation. A different approach to the measurement of signal attenuation due to rock samples is to pass them through a non-radiating slot in a waveguide structure. Slots can be cut into waveguide walls in such a way that little or no energy is radiated out of the slot. A non-radiating slot was required in this application to ensure maximum signal transmission through the waveguide.

The dimensions of fundamental mode (TE_{10} mode) rectangular waveguides in the microwave frequency range are physically too

small to allow a large enough slot in them through which rock samples could be passed. In order to have a large enough non-radiating slot in a waveguide without going too low in frequency where the loss would be very small it was decided to consider the use of overmoded waveguides.

A frequency of 3GHz was chosen for experimentation because the waveguide is comparatively large at this frequency and the loss is also quite large. The waveguide does not have to be overmoded too many times to produce a structure with a large enough slot through which rock samples could be passed.

4.2.1 Construction of 3GHz waveguides

A 3GHz fundamental mode (TE_{10} mode) and 3 times overmoded (TE_{30}) rectangular waveguide were built for comparison. These waveguides were constructed from stiff cardboard lined with aluminium cooking foil for ease of construction.

The E field distributions in TE_{10} and TE_{30} mode rectangular waveguides are shown in figure 4.14.

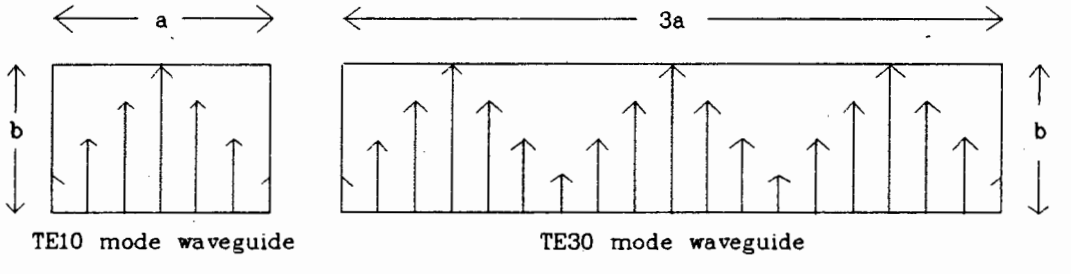

Fig. 4.14 E field distribution in TE_{10} and TE_{30} waveguide.

The TE_{10} mode waveguide had a 10cm long and 0.5cm wide

non-radiating slot cut through the centre of both its broad walls as shown in figure 4.15.

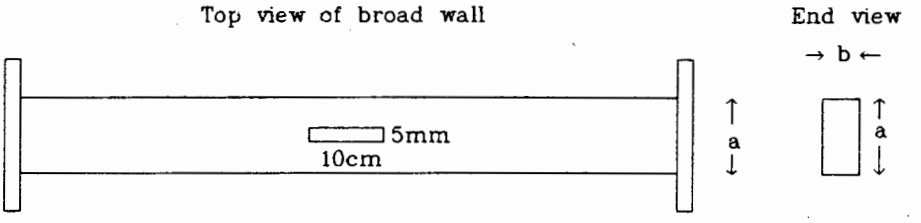

Fig. 4.15 3GHz TE_{10} mode waveguide with non radiating slot.

The TE_{30} mode waveguide was constructed as shown in figure 4.16. The slots in this waveguide were placed in the centre of the broad walls and were 10cm long and 7cm wide to allow rock samples to pass through the structure.

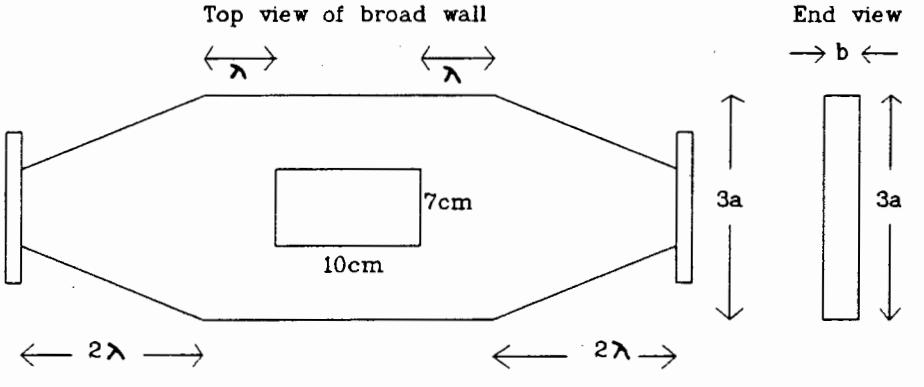

Fig. 4.16 3GHz TE_{30} mode waveguide with non radiating slot.

Both the TE_{10} and TE_{30} waveguides had flanges at either end for coupling to coaxial cable to rectangular waveguide transformers. The TE_{30} waveguide had a 2λ long tapered section at either end to form a gradual transition from TE_{10} dimensions to TE_{30} dimensions.

Screws were placed into the broad wall at the required points to ensure the propagation of only TE_{30} mode. The removal of these screws did not seem to make any difference to the received signal level.

The ends of the tapered waveguide sections form discontinuities in the waveguide. Hence 1λ long sections of TE_{30} waveguide were included at the ends of the tapered section to ensure that only TE_{30} mode was propagating across the slotted section of the overmoded waveguide. The overall length of the waveguides in figures 4.15 and 4.16 were identical to allow comparative measurements to be made.

4.2.2 Results

The insertion loss due to the TE_{30} mode waveguide was found to be 1dB greater than that of the TE_{10} mode waveguide. This was due to a small amount of signal radiation from the large slots in the TE_{30} mode waveguide. The insertion loss for the two waveguides was equal when the slots in the TE_{30} mode waveguide were temporarily covered with aluminium foil.

A 7cm square of attenuative card was alternatively inserted into the slots in the two waveguides and passed through them. This produced an insertion loss of 18dB in the TE_{10} mode waveguide and 7dB in the TE_{30} mode waveguide. Some variation of the attenuation through the the TE_{30} mode waveguide was observed when the position of the lossy card was changed in the slot. This phenomenon was due to the varying amount of E field intersected by the card and discontinuity effects at the end of the slot. Note that the energy density in the TE_{30} mode waveguide is lower than in the TE_{10} mode waveguide.

Figure 4.14 indicates the E field distribution across the waveguides. It can be seen that the narrow slot in the centre of the TE_{10} mode waveguide will have a fairly constant E field distribution across the slot whilst the TE_{30} mode waveguide will have a more widely varying E field distribution across the width of the slot.

When samples of gabbro and kimberlite were inserted into the slot in the TE_{30} mode waveguide the amounts of signal attenuation observed were too low to effect rock differentiation. This was expected in the light of the above results with more signal passing around the rock samples in the waveguide rather than being attenuated by the samples.

The use of higher frequency overmoded waveguides was not considered viable because these would have to be overmoded many times to produce a structure of suitable physical dimension. For example, a 10GHz TE_{10} mode waveguide would have to be overmoded ten times to produce a structure of similar physical dimension to the TE_{30} mode 3GHz structure. The low energy density and complex field distribution of such a high order mode waveguide would result in undesirably low values of signal attenuation due to rock samples.

It was therefore concluded that overmoded waveguides used in the above manner are not a practical means for distinguishing between different rock types on the basis of signal attenuation. The alternative technique of passing the rock types between two small antennas where the rocks obstruct the microwave beam and introduce signal attenuation was considered to be a much better method.

4.3 Investigation of microwave signal reflection from rock samples

If two different rock types exhibited a consistently detectable difference in reflected signal at a particular frequency then this fact could be used to devise a rock differentiation system using that microwave frequency.

Microwave signal reflection from a rock will be affected by the geometry of the rock. The size of the rock will have a bearing on the amount of signal reflected from its surface. The shape of a rock will influence the reflected signal from the rock and a rough surfaced, irregular shaped rock may cause signal scattering to occur. The dielectric properties of the rock will also influence the amount of signal reflection from the rock.

To reduce the effect of the above mentioned factors, flat sided rock samples were examined to accurately determine the reflected signal levels from the different rocks.

4.3.1 Equipment used for reflection measurements

A 10.55 GHz intruder alarm oscillator with a neighbouring detector diode was used to irradiate rock samples as shown in figure 4.17.

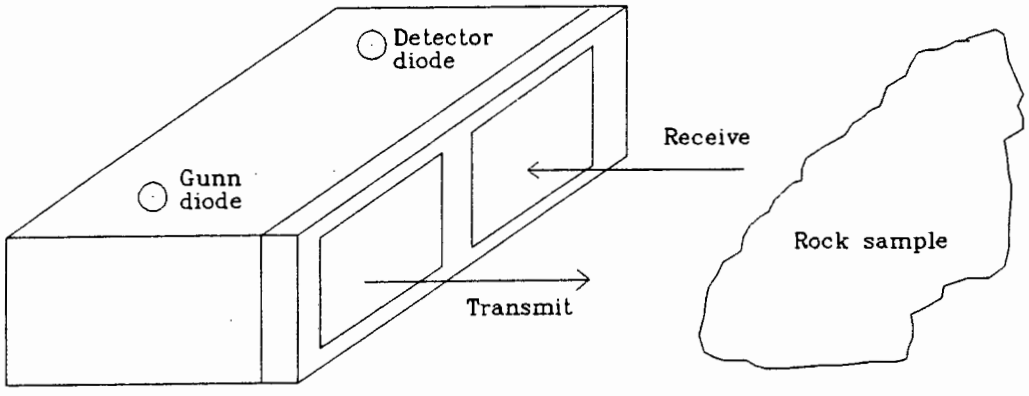

Fig. 4.17 10.55 GHz transmitter and receiver.

The circuit diagram of the connections to the Gunn oscillator and detector diode is given in figure 4.18. The output from the detector diode was observed on an oscilloscope.

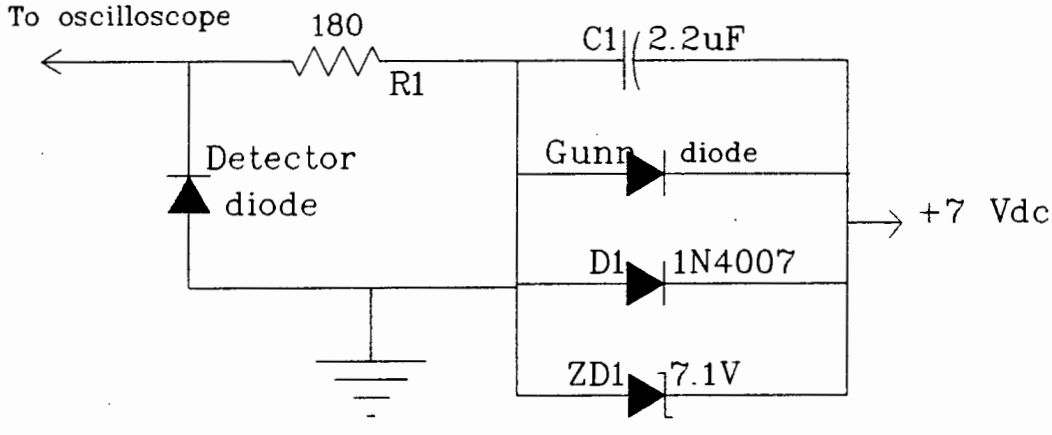

Fig.4.18 Circuit connections of 10.55 GHz test equipment.

4.3.2 Results of reflection measurement tests

Flat sided samples of gabbro and kimberlite and a 0.5cm thick aluminium plate were used for comparative measurements. Measurements were repeated at different distances from the transmitter/receiver. The results shown in figure 4.19 were obtained using the equipment described in section 4.3.1.

Reflective object	Detector voltage with objects at the antenna	Detector voltage with objects 3.5 cm from the antenna
No object	0.0 V	0.0 V
5mm aluminium plate	0.8 V	1.5 mV
12cm thick Gabbro	0.15 V	0.5 mV
12cm thick Kimberlite	0.18 V	0.5 mV

Fig. 4.19 10.55 GHz reflection measurements.

From the results in figure 4.19 it can be seen that the equipment was operating correctly with no detected signal with no reflective object in front of the antenna and the maximum reflected signal with a conductive metal plate in front of the antenna. the surface area of the metal plate exposed to the microwave signal was similar to the exposed surface area of the gabbro and kimberlite samples.

The data indicate that the reflected signal level from the gabbro and the kimberlite were very similar and that both rock types reflect considerably less signal than the

metal plate. There was no detectable variation in reflected signal level as the antenna was moved across the face of either rock type. The received signal level dropped as the sample was moved away from the antenna.

Rough surfaced and randomly shaped rock samples were also examined in various orientations. Minor variations in received signal level were observed as these samples were rotated but the comparative signal levels from gabbro and kimberlite remained the same. The overall received signal levels from the irregular shaped rocks were lower than from the flat rocks due to signal scattering. The signal level was strongly dependent on the orientation of the rocks.

The above results indicated that gabbro and kimberlite reflect very similar levels of microwave power. In practice the moisture content of the rocks will vary and the rocks will be coated with mineral slimes further affecting the measurements. It was therefore shown that microwave signal reflection cannot be used to differentiate between samples of gabbro and kimberlite. The signal reflection was found to be more a function of the rock shape than the rock type.

4.4 Conclusions

As a result of the findings of this section, the following conclusions can be drawn:

1. The use of reflected microwave signals from gabbro and kimberlite is not a practical means of distinguishing between rock types in the static case.

2. The use of microwave signal transmission through overmoded waveguide structures,as discussed in section

4.2, cannot be used as a means of differentiating between gabbro and kimberlite.

3. There is a detectable difference in microwave signal attenuation between samples of kimberlite and the waste rocks gabbro and felsite, when the rock samples are placed between a transmitting and a receiving antenna.

4. To obtain accurate signal attenuation measurements through rock samples,using two antennae, it is essential that no signal can pass directly between the antennae when a rock is positioned between them.

5. The microwave signal attenuation through kimberlite increased with increasing frequency and the difference in attenuation between kimberlite and the waste rock increases with increasing frequency therefore it appears that a high operating frequency should be chosen for most reliable rock differentiation. This has the added advantage that the microwave antennas become smaller at the high frequencies, thus smaller rocks can be sorted and chance of signal creepage decreases.

6. The construction of a high frequency microwave transmitter and receiver is justified in the light of the above results.

5. DESIGN OF MICROWAVE TRANSMITTER AND RECEIVER

The investigation of microwave signal attenuation between two antennae due to the presence of rock samples as described in section 4.1, revealed that there was a detectable difference in signal attenuation between the different rock types over a broad frequency range. It was therefore decided to construct a microwave transmitter and receiver for further laboratory testing of signal attenuation due to the presence of rock samples.

The transmitter and receiver had to built in such a way that rock samples could be passed between the antennae. The transmitter and receiver were therefore housed in different cabinets as shown in figure 5.1.

Fig. 5.1 The transmitter and receiver.

A different version of the equipment was constructed with remote antenna housings for mounting above and below a

conveyor belt as shown in figure 5.2. This system was used for dynamic measurements of signal attenuation due to rock samples.

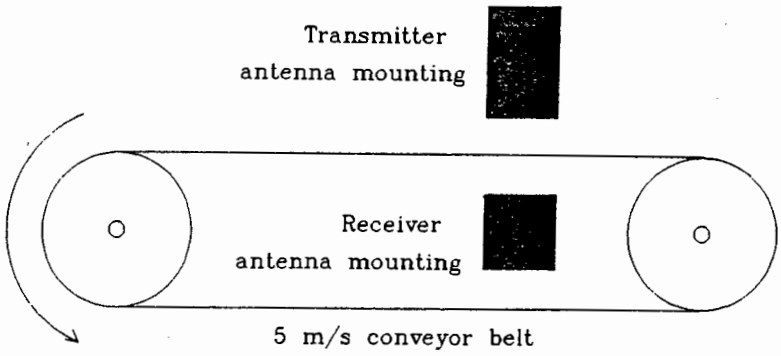

Fig. 5.2 Mounting of remote antennae.

The remote antenna housing illustrated in figure 5.2 had to be moisture proof , dust proof and have negligible insertion loss at the chosen operating frequency. Sealed plastic containers were chosen to protect the antennae. The microwave signals passed virtually unaffected through these containers. Although the optimum container wall thickness for maximum signal transmission would be a radome thickness of $n*\lambda\backslash 2$ where n = 1,2,3... this was not found necessary due to the low loss nature of the plastic containers.

The choice of operating frequency was influenced by a number of factors. The size of rocks to be examined relative to the antenna aperture size was an important factor to be considered. If a low operating frequency with larger antenna was chosen then the system would be limited to use with large rock samples. This is due to the fact that the smallest rock sample to be detected must completely cover the antenna aperture for the system to function correctly.

Microwave frequencies with resonant moisture absorption peaks were to be avoided for the reasons mentioned in section 3.1. The attenuation difference between gabbro and kimberlite at the chosen operating frequency was also considered.

It was decided to construct the transmitter and receiver so that different microwave sources and detectors could be driven from the same circuit. This allowed an examination of different operating frequencies without unnecessary circuit duplication.

A decision had to be made between continuous wave (CW) operation and pulsed mode operation. If the transmitter were used in CW mode then the receiver detector diode would function as a simple direct current rectifier. This would require dc amplification which is prone to dc offset and drift. The expected signal input at the receiver is in the region of 10 μV and 5 mV and dc offsets or drift in this case could cause serious errors.

The solution to this problem is to use pulsed mode operation where pulses of microwave signal are transmitted. This is advantageous because the receiver can then be designed to avoid any dc amplification and thereby eliminate many of the possible errors involved with dc amplification. A pulsed transmitter was fabricated for this reason.

A decision had to be made between powering the transmitter and receiver from batteries or the mains supply. Mains operation was chosen due to the current requirements of the transmitter and to avoid the problem of battery maintenance. The pulsed operation of the transmitter may cause supply voltage spikes and variations. To prevent this from adversely affecting the operation of the receiver, separate power supplies were used for the transmitter and the receiver. These were housed in separate shielded containers.

5.1 Description of transmitter circuitry

A block diagram of the transmitter is shown in figure 5.4. It

can be seen that the transmitter circuit consists of a 1kHz oscillator followed by an adjustable attenuator. This facilitates adjustment of the amplitude of the oscillator output voltage. The attenuator output is coupled to a current driving stage which in turn drives a Gunn oscillator. The circuit has been designed to provide a wide range of output voltages in order to be able to drive a variety of different Gunn oscillators.

A circuit diagram of the transmitter is shown in figure 5.5. The heart of the transmitter circuit is a 1kHz square wave oscillator with a 50% duty cycle. This oscillator is realized using a LM555 timer chip. The resistors R1 and R2 and capacitors C1 and C2 were chosen to provide a 50% duty cycle and a 1kHz oscillation frequency as shown in fig 5.3.

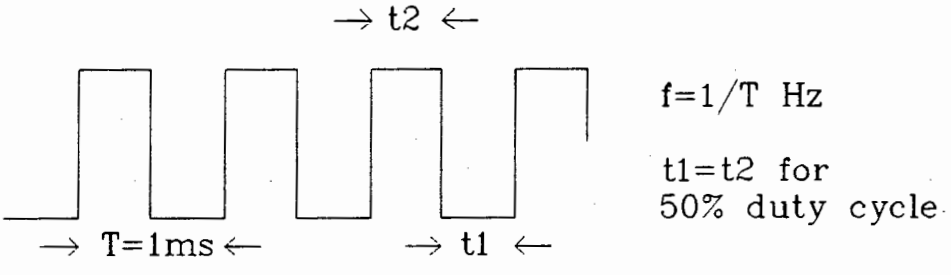

Fig. 5.3 50% duty cycle 1KHz square wave.

The choice of the 1kHz oscillation frequency is arbitrary but should be low enough to avoid any high frequency limitations in the following stages of the circuit.

The duty cycle of 50% was deliberately chosen because this allows a smooth 1kHz sinewave (fundamental of the square wave) to be obtained in the receiver unit by means of bandpass filtering. The capacitors C3 and C4 are power supply decoupling capacitors. Capacitor C3 is included for supply smoothing while the smaller capacitance C4 will filter any sudden high frequency spikes that cannot be smoothed out by

the larger and slower responding C3.Supply decoupling capacitors C5, C6, C8 and C9 were connected in pairs across the voltage supply rails as indicated in figure 5.5.

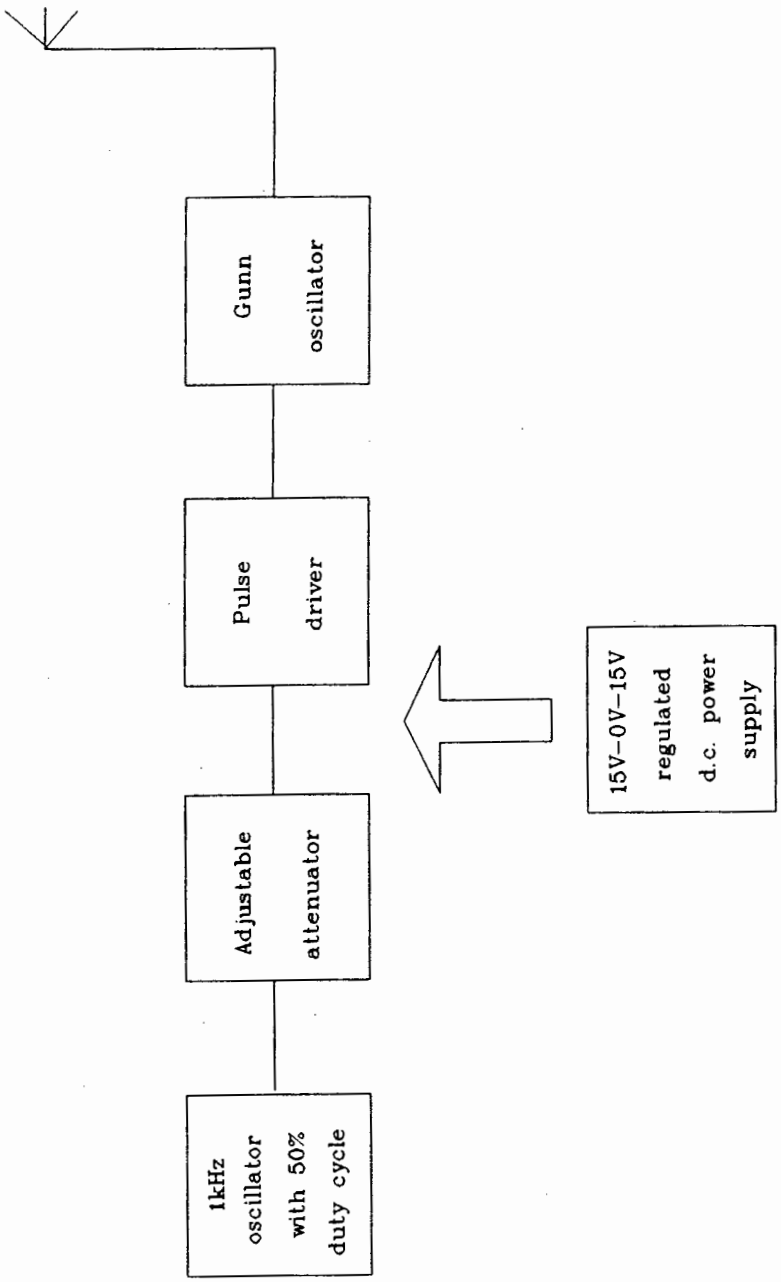

Fig. 5.4 Block diagram of transmitter circuit.

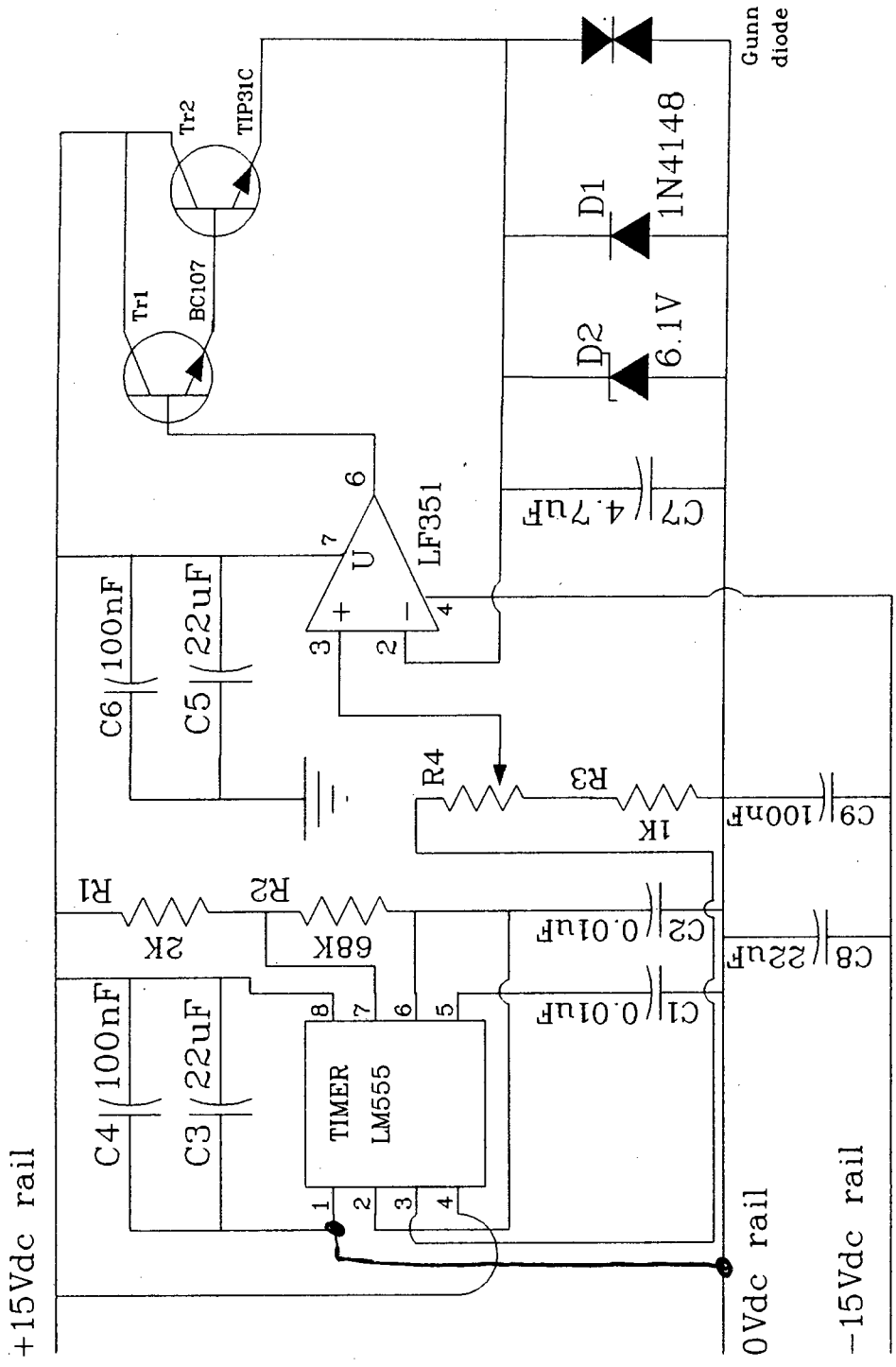

Fig. 5.5 Transmitter circuit diagram.

The output of the LM555 oscillator is fed to an attenuator R4 to facilitate amplitude adjustment of the 1kHz square wave.

The LM555 chip only has to deliver a few milliamps of current to the attenuator so that problems should not occur with the temperature stability of this component.

The square wave signal from the attenuator is fed into the non-inverting input of the LF351 operational amplifier. This op.amp. is configured as a non-inverting follower whose output is used to drive the base of Tr1, a BC107 small signal transistor. The transistors Tr2, a TIP31C power transistor, and Tr1 are connected in a Darlington configuration to form a high gain output module capable of delivering an output current in excess of 1 ampere. The inverting input of the op. amp. is connected to the emitter of Tr2. This negative feedback configuration improves the switching speed of the circuit.

The operational amplifier, Tr1 and Tr2 form the pulse driver stage of the circuit. Output currents of up to 1 ampere may be required to drive a Gunn oscillator. The output of the operational amplifier can only supply a few milliamperes of output current. This is insufficient to drive the base of Tr2 directly hence the Darlington transistor configuration is used. The operational amplifier can easily drive Tr1 which in turn can drive Tr2.

In this way a variable voltage 1kHz oscillator is formed with the ability to deliver a high output current. The TIP31C was well heatsinked and can continuously deliver up to 3 amperes of current. The Gunn oscillators used required less than 1 ampere of current. Test loads drawing a current of one ampere were connected to the circuit for up to 24 hours to test it for output voltage droop. No output voltage droop was detectable after a 24 hour period.

The Gunn oscillator is connected between the emitter Tr2 and the ground rail, as shown in figure 5.5. Capacitor C7 is

connected across the Gunn oscillator terminals to improve the stability of the circuit. The zener diode D2 is connected across the Gunn oscillator to prevent it from being damaged by a possible voltage spike. Diode D1 is connected across the Gunn oscillator terminals to protect it from the possibility of becoming reverse biased when the voltage supply is switched off.

The rise time of the pulses applied to the Gunn oscillator is an important factor related to the frequency stability of the oscillator. The rise time of the pulses should be as short as possible to reduce the frequency drift of the oscillator. In this application, however, absolute frequency stability is not really required. The amplitude of the received signal will be more important than the exact frequency of the signal.

The output waveform of this circuit was examined on an oscilloscope when delivering an output current of 1 ampere. The pulse rise time was approximately 10 ms. This is small compared to the 500ms pulse width and is adequate in this application.

The transmitter circuit is figure 5.5, with the exception of the Gunn oscillator, was mounted on a printed circuit board that was designed to accommodate it. A copy of the printed circuit board foil pattern is given in Appendix C.

5.1.1 The Gunn oscillator

The Gunn oscillators used in this transmitter are commercially manufactured varactor tunable units. The X band Gunn oscillator required a 10 Vdc supply and the 35GHz Gunn oscillator required a 6 Vdc supply. The attenuator shown in figure 5.5 was adjusted to suit the oscillator used. The Gunn sources were connected to

square waveguide antennae as shown below in figure 5.6.

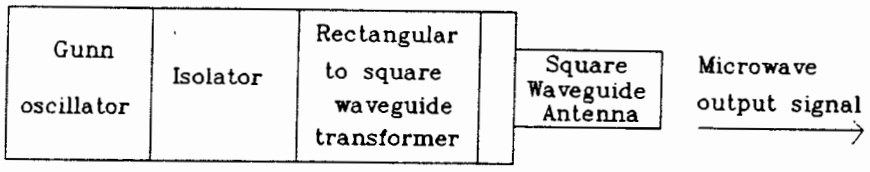

Fig.5.6. Connection of Gunn oscillator to antenna.

An isolator was connected to the source to prevent any possible impedance mismatch due to the presence of a rock sample, from reducing the output power or even causing the Gunn oscillator to switch off and stop oscillating. The rectangular to square waveguide quarter wavelength transformers and square waveguide antennae were designed as described in section 4.1.1. Antenna dimensions and dimensions for the rectangular to square waveguide transformers are included in Appendix B.

5.1.2 The transmitter power supply

The transmitter circuit described in section 5.1 requires voltage supply rails of +15V, -15V and 0V for correct operation. A circuit diagram of the transmitter power supply is shown in figure 5.7.

A mains switch is used to switch the mains supply live and neutral wires which are connected across the primary windings of the mains stepdown transformer. The transformer primary is protected against current overload by means of a series connected 1 A fuse.

The centre tapped secondary winding of the mains transformer is adequately rated at 18V-0V-18V at 1.5

amperes. The output from the transformer is rectified by means of a bridge rectifier that can safely deliver a current of 2 A without destruction. The centre tap on the transformers secondary winding is connected to ground.

Both the positive and negative outputs of the bridge rectifier are smoothed using two parallel connected 2200µf electrolytic capacitors rated at 40 V each. Capacitors C5 and C6 are small 220 pf ceramic capacitors connected in parallel with the large 2200µf smoothing capacitors to eliminate any high frequency voltage spikes that may occur.

The capacitively smoothed rectifier outputs are then fed into voltage regulators. The positive output of the rectifier is connected to a 7815 voltage regulator to provide a stable +15V supply rail. The negative output of the rectifier is connected to a 7915 voltage regulator to provide a stable -15V supply rail. These voltage regulators can provide output currents of up to 1.5A each and are adequately heatsinked to improve thermal dissipation.

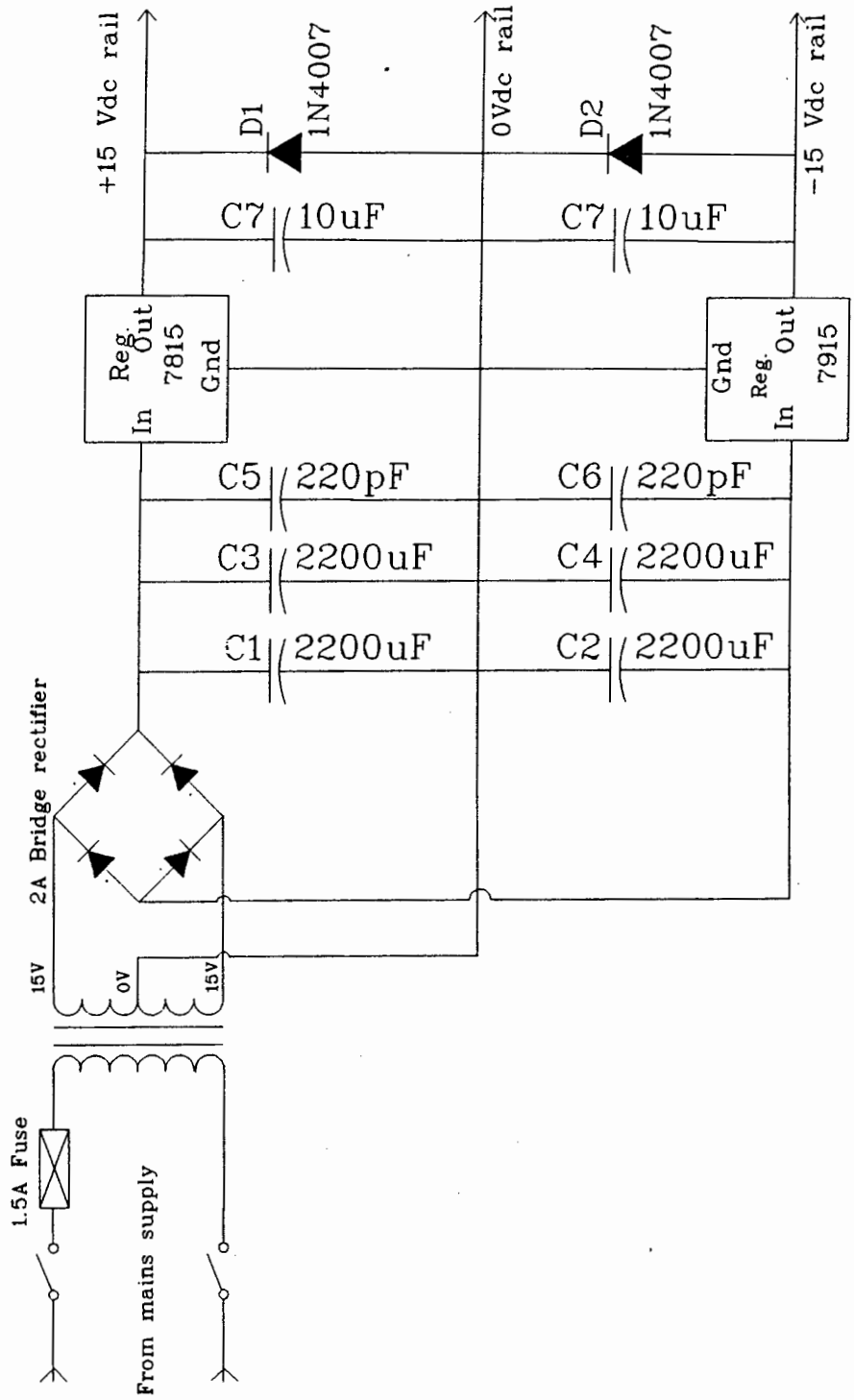

Fig.5.7 Circuit diagram of transmitter power supply.

Capacitors C7 and C8 are 10 μF tantalum capacitors connected between the voltage regulator outputs and the ground rail to ensure smoothing of the 15V dc rails in the event of a voltage spike or dip occurring. The diodes D1 and D2 are connected between each voltage regulator output and the ground rail. These diodes provide output short circuit protection for this power supply.

5.2 Description of receiver circuitry

Two different receiver modules were constructed for experimentation. The block diagram of figure 5.9 indicates a receiver to provide an indication of the rock type by means of the deflection of a moving coil meter. The modified receiver block diagram shown in figure 5.10 indicates a receiver to provide a continuous dc output voltage in the range 0-5 Vdc for interfacing to an A/D card to facilitate data capture in a personal computer.

The modulated microwave signal from the transmitter was detected using the configuration shown in figure 5.8.

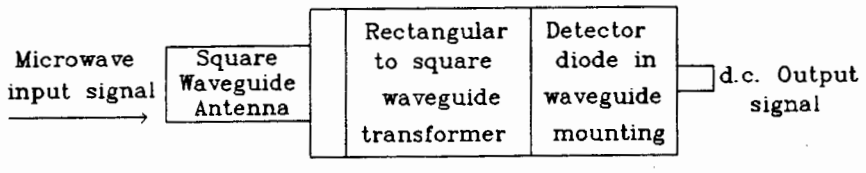

Fig. 5.8 Detector diode mounting and antenna.

The microwave input signal is received via the square waveguide antenna. This is connected to a detector diode mounted in a rectangular waveguide cavity via a rectangular to square waveguide transformer. This transformer and antenna

are identical to those discussed in section 4.1.1.

The receivers were designed in such a way that detector diodes of different frequencies with their respective antennae, can be used interchangably in the circuit. From the block diagrams of figures 5.9 and 5.10 it can be seen that the output from the detector diode is first amplified and then bandpass filtered before undergoing further amplification. The detector diode output will be a 1kHz square wave if the transmitter of section 5.1 is used. The amplitude of this square wave is less than 10 mV. The first stage of amplification amplifies this square wave by 40dB.

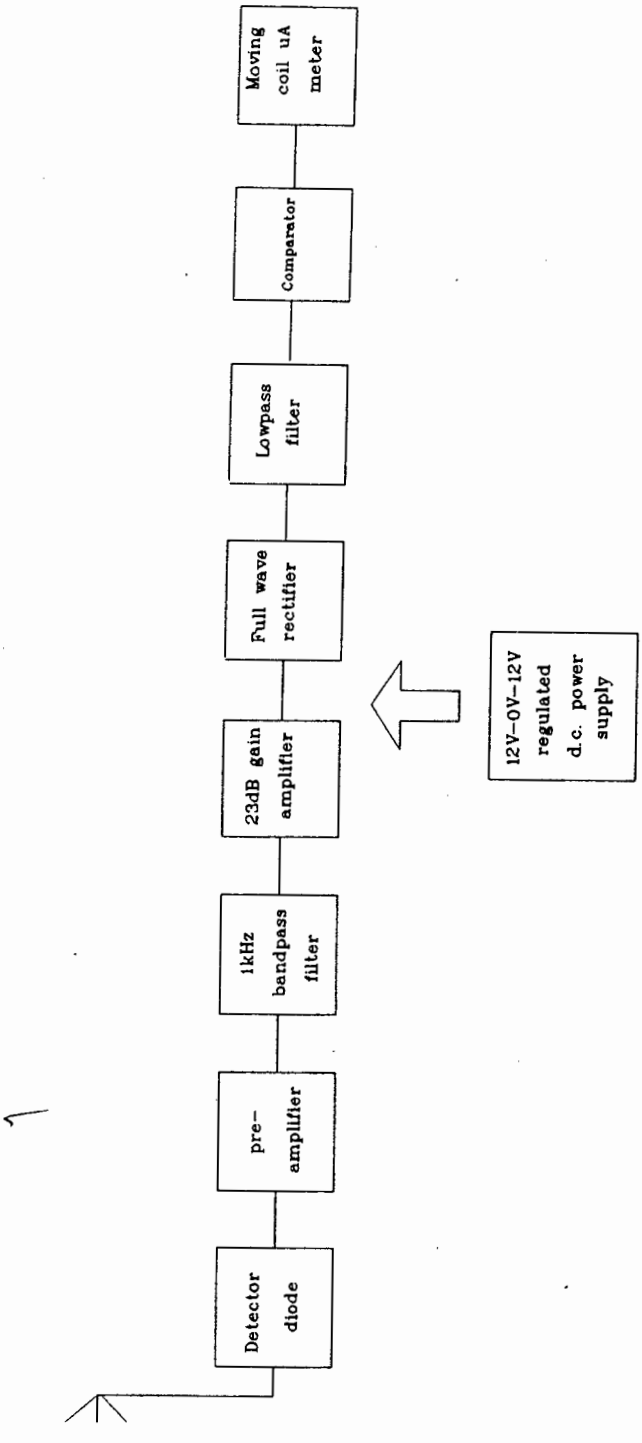

Fig. 5.9 Block diagram of receiver circuit with moving coil meter.

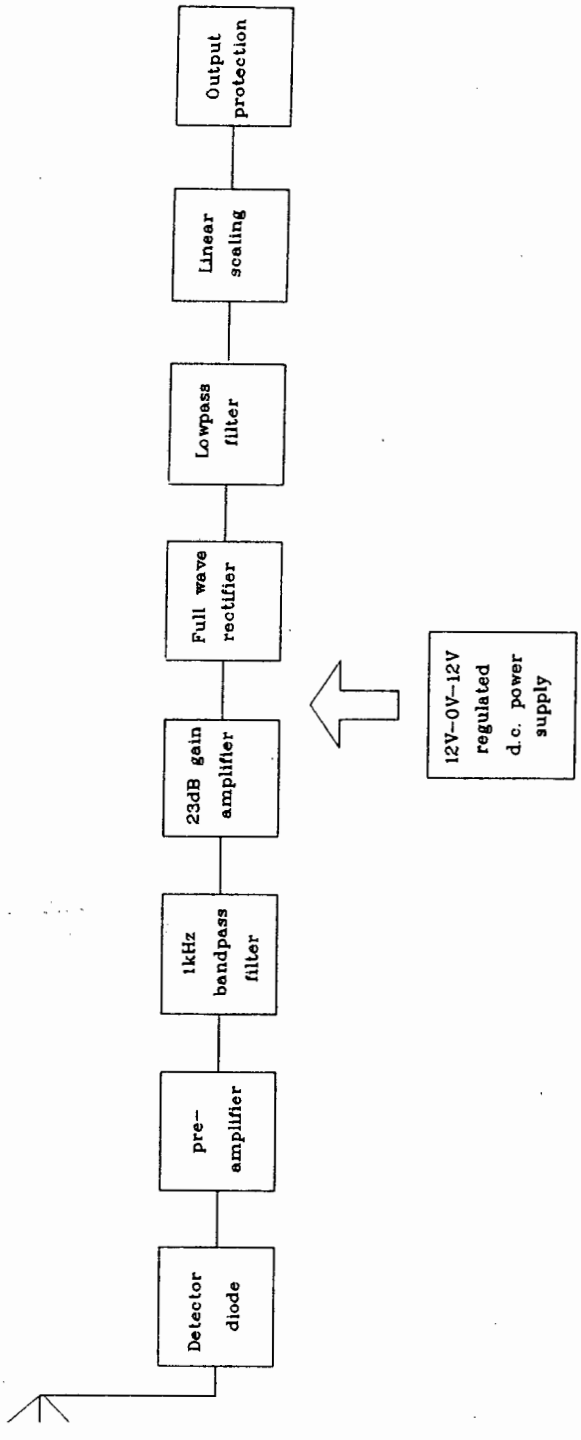

Fig. 5.10 Block diagram of receiver circuit with 0 - 5 Vdc output.

The bandpass filter centred at 1KHz extracts the 1KHz sinewave fundamental from the squarewave. The sinewave is then amplified and rectified using a full wave rectifier. The output of the full wave rectifier is low pass filtered to produce a dc level. The two receiver designs of figure 5.9 and 5.10 are identical up to this point.

The receiver of figure 5.9 uses this dc signal to trigger a comparator which is set to deflect a moving coil microampere meter. If a large signal is received then the dc level will be high and the comparator will not cause the meter to deflect. The samples of gabbro allow a large microwave signal to reach the receiver. The samples of kimberlite attenuate the signal more than the gabbro and will therefore only allow a small signal to arrive at the receiver. When the comparator trigger level is correctly set it can be used to deflect the meter in one of two states. Signals above the comparator level indicate low attenuation and signals below the comparator level indicate high attenuation.

The receiver of figure 5.10 feeds the output of the lowpass filter into a linear scaling circuit to produce a continuous dc output voltage the range 0-5Vdc. This output is suitable for interfacing to a personal computer via an A/D convertor card. Output protection is included to prevent possible damage to the A/D convertor in the unlikely event of equipment breakdown.

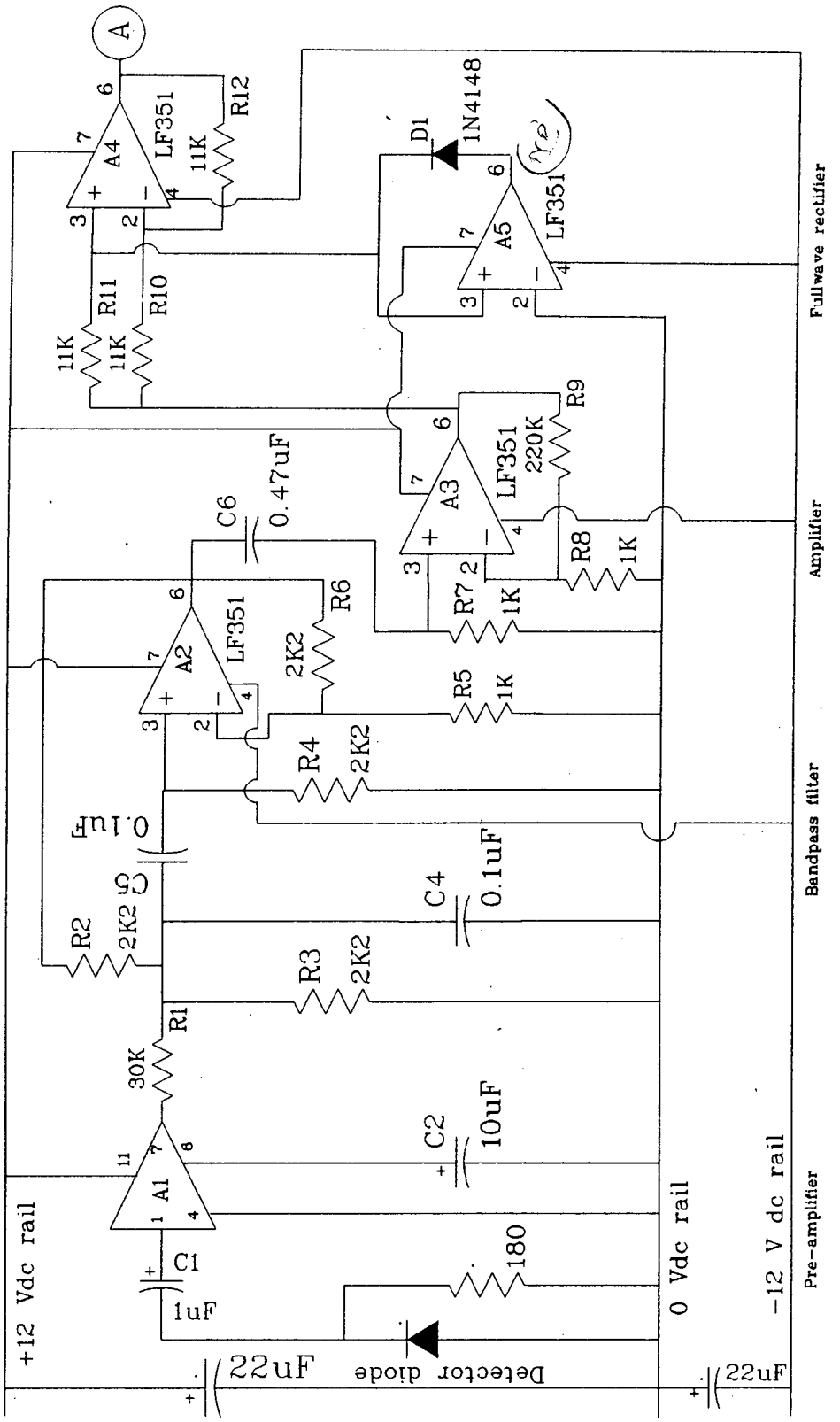

Fig. 5.11a Initial stages of receiver circuit.

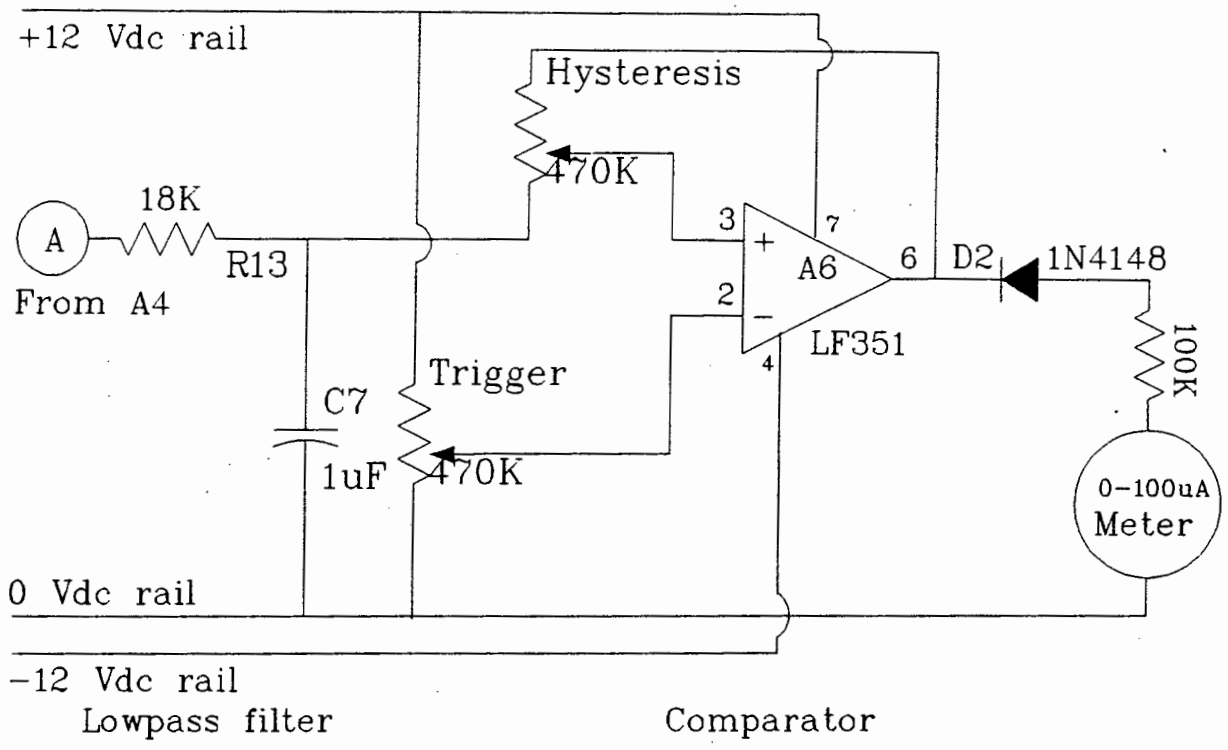

Fig. 5.11b Final stages of receiver with moving coil meter.

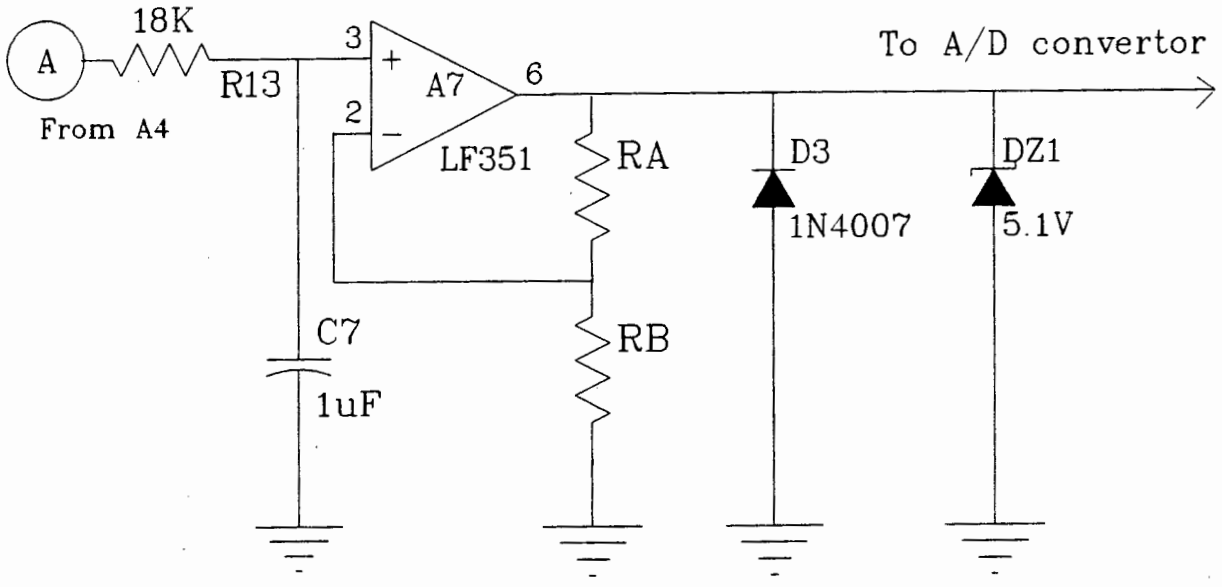

Fig. 5.11c Final stages of receiver circuit with 0-5 Vdc output.

A circuit diagram of the receiver up to the full wave rectifier is shown if figure 5.11a. The final stages of the receiver circuit using the meter and comparator is given in figure 5.11b. Figure 5.11c illustrates the final stages of the receiver circuit with the linearly scaled 0-5 Vdc output.

It can be seen from figure 5.11a that the detector diode output is ac coupled to amplifier A1 via capacitor C1. The amplifier A1 is a LM382 low noise preamplifier and has been configured to give a voltage gain of 40dB. This voltage gain is achieved by connecting capacitor C2 between pin 6 and ground. A high quality tantalum capacitor was used here to try to improve long term gain stability.

The preamplifier is designed to operate from a single supply so that it's output has a large (approximately 6Vdc) offset to ensure a good signal voltage swing. This chip was used due to its good noise performance. The dc offset at its output was eliminated by means of the following bandpass filter.

The active bandpass filter is formed by R1, R2, R3, R4, R5, R6, C4, C5 and A2. The filter was designed to have a centre frequency of 1kHz and a bandwidth of 200Hz with unity gain. The following design procedure was used:

$Q_p = f_o/B = 5.1$ and $w_p = 2\pi f_o = 6408.8$ radians/second where $f_o = 1$kHz so $w_p/Q_p = 1256.6$.
The desired transfer function is

$$T(s) = \frac{1256.6s}{s^2 + 1256.6s + 4.1 \times 10^7}$$

Now let C4 = C5 = 1F and
let $R1 = R2 = R4 = \sqrt{2}/w_p = 2.21 \times 10^{-4}\Omega$

$R6/R5 = 3-\sqrt{2}/\omega_p Q_p = 2.723.$

These values are then scaled in amplitude by a factor of 10^7 to give:

C4 = C5 = 0.1μF and R1 = R2 = R4 = 2210Ω

Let R5 = 1kΩ then R6 = 2723Ω

The gain factor $K = \omega_p(2\sqrt{2} - 1/Q_p) = 16870.2$

but K must be $= \omega_p/Q_p = 1256.6$

so the attenuator consisting of R1 and R3 is used to arrange this

$R3/R1 = R3' = 0.0745$

so R1 = 29664Ω

and R3 = 2388Ω

The values shown in fig.5.11 are the closest manufactured values available. This design process is detailed on page 287 of [11].

The bandpass filter was tested separately and the centre frequency was found to be 962Hz. The 3dB cutoff points were 847Hz and 1111Hz. The difference in centre frequency between the theoretical and measured values is due to rounding off the component values. A LF351 operational amplifier is used for A2 and the rest of the operational amplifiers in the receiver circuit. The output from the bandpass filter is ac coupled to the next stage of amplification via capacitor C6.

The non inverting amplifier A3 is used to amplify the 1kHz sinewave signal from the bandpass filter. Resistor R7 is used to provide a dc bias path for this ac coupled stage. The gain of this stage is determined by the resistor ratio R8 + R9/R8. A gain of 23dB was selected.

The amplified sinewave is then full wave rectified using an "optional inverter" configuration that is switched using an active clamp. Precision 2% tolerance resistors were used for R10 and R12 to ensure accurate rectification. The active

clamp is formed by A5 and D1. The optional invertor is formed by amplifier A4. This active rectifier circuit should not introduce any errors due,for example, to diode voltage drops. The rectified sinewave signal is then filtered with the low pass filter formed by R13 and C7. This filter has a time constant = 0.018 seconds.

For the receiver outlined in figure 5.9 this dc signal is fed into the comparator circuitry of figure 5.11b. The comparator is formed by an operational amplifier A6 configured to have an adjustable amount of positive feedback for hysteresis. This adjustment is realized by varying R14. The variable resistor R15 is adjusted to change the trigger level of the comparator.

The output of the comparator is connected to an ammeter with 100 mA full scale deflection. A 100 KΩ series resistor is connected between the ammeter and the comparator to limit the current flow to the meter. The diode D2 is connected so that the meter will deflect when the input to the comparator is small.

The components in this receiver circuit, with the exception of the detector diode and the meter. were all mounted on a printed circuit board specifically designed to accommodate it. A copy of the printed circuit board foil pattern is given in Appendix C.

For the receiver outlined in figure 5.11c, the dc signal is fed into an operational amplifier A7. The variable resistors RA and RB were adjusted so that the output of A7 was a linearly scaled version of its input but limited to the range 0 - 5 Vdc. The output of A7 was then connected to an A/D convertor to provide data to a personal computer.

The zener diode DZ1 was included to provide overvoltage protection to the equipment connected to the output of this

circuit. The diode D3 was connected to the output of A7 to preclude the possibility of a negative output voltage as this could damage equipment connected to this circuit. The circuit in figure 5.11c was constructed on Veroboard.

5.2.1 The receiver power supply

A bipolar voltage supply was required to drive the circuitry in the receiver. The 12V rails were chosen for convenience and due to the availability of a suitable transformer. A circuit diagram of the receiver power supply is shown in fig. 5.12.

The primary side of the mains stepdown transformer is connected to the mains supply via a switch and a 1A fuse. The secondary winding is centre tapped and the centre tap is grounded. The output from the 2A rated secondary winding is full wave rectified using a 1A bridge rectifier. The positive output of the rectifier is used to create the positive voltage rail and the negative rectifier output is used to create the negative voltage rail. Capacitors C1 and C2 are 2200µF electrolytic capacitors connected between the voltage rails and ground for smoothing. Capacitors C3 and C4 are small 220pf ceramic capacitors connected in parallel with the large smoothing capacitors to eliminate any high frequency voltage spikes that may occur.

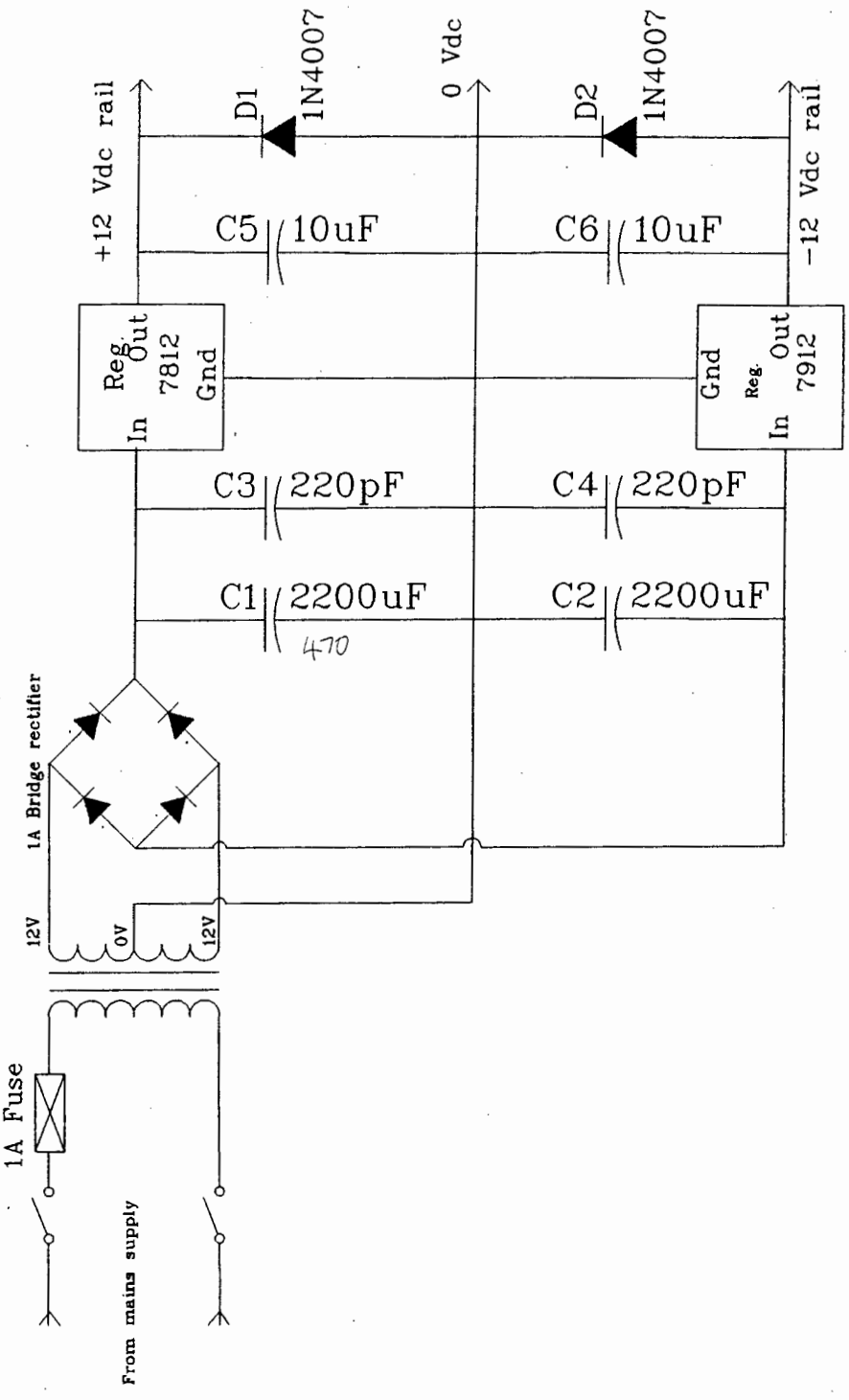

Fig. 5.12 Receiver power supply.

The smoothed rectifier outputs were then connected to voltage regulators. A 7812 voltage regulator was used to create the +12V supply rail and a 7912 voltage regulator was used to from the -12V rail. The voltage regulators were heatsinked to improve thermal dissipation. The receiver circuit should draw less than 20mA from each supply rail. The voltage regulators are safely rated and can deliver 1A each if required.

The tantalum capacitors C5 and C6 are connected between the voltage regulator outputs and the ground rail to ensure smoothing of the 12Vdc rails. The diodes D1 and D2 are connected between each voltage regulator output and the ground rail. These diodes provide output short circuit protection for this power supply.

The components for this power supply, with the exception of the transformer fuse and switch, are all mounted on a printed circuit board specifically designed for it. A copy of this printed circuit board foil pattern is included in Appendix C.

6. RESULTS

The equipment described in section 5 was fabricated and extensive tests were performed with these production model microwave transmitters.

6.1 Static results

The use of different frequency microwave components was examined. 10GHz and 35GHz microwave components were tested. Rotary vane attenuators for use at these frequencies were connected to the receivers as shown in figure 6.1. Note that an isolator is included at the receiver to eliminate the effect of possible detector impedance mismatching.

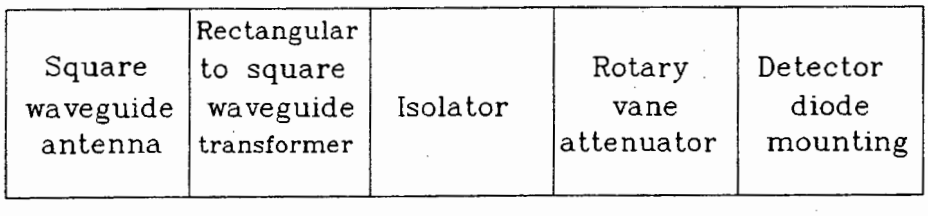

Fig. 6.1 Connection of Rotary Vane Attenuator to receiver.

The rotary vane attenuators were used to obtain a reading of insertion loss due to rock samples, directly in dB. The detector diodes output was observed on an oscilloscope. The rotary vane attenuator was set to 0 dB attenuation and a rock sample was inserted between the transmit and receive antennae. The received signal level on the oscilloscope was observed and then the rock sample was removed. The rotary vane attenuator was then used to reduce the received signal level to that observed due to the presence of the rock sample. The attenuation due to the rock sample was then read off of the attenuator directly in dB.

The results at 10 GHz were similar to those shown in figure 4.11. This indicated that the 10GHz equipment was functioning correctly. The 35GHz units with their reduced antenna aperture area, useful when differentiating between small rocks, yielded the promising results shown in figure 6.2.

Rock type	Average attenuation in dB/cm
Kimberlite	9.33 dB/cm
Gabbro	2.38 dB/cm

Fig. 6.2 Average attenuation at 35GHz.

It can be seen that there is a detectable difference in signal attenuation between gabbro and kimberlite at 35GHz. The attenuation through each rock type was higher at 35GHz than at 10GHz. The difference in signal attenuation between gabbro and kimberlite was higher at 35GHz than at 10GHz. This factor, together with the advantage of small antenna aperture area for detection of small rocks, indicated that 35GHz was the better operating frequency.

A 60GHz Gunn oscillator was made available for experimentation. The use of such a high frequency system has the advantage of very small aperture antennae, allowing detection of very small rock samples. As mentioned in section 2.1 the microwave signal attenuation through a medium increases proportional to the square root of the frequency. It was found that the overall signal attenuation at 60GHz was too high to effect reliable rock differentiation using the equipment discussed in section 5,and the signal level at the receiver was too small to detect.

6.1.1 Examination of signal attenuation through gabbro

Some irregularities were observed with microwave signal attenuation through samples of gabbro. Flat, parallel sided samples of gabbro placed between the antennae and perpendicular to them, exhibited low signal attenuation. The attenuation due to the gabbro sample appeared to vary as the orientation of the sample was changed. It was found that the signal attenuation due to randomly shaped gabbro samples was also dependent on orientation. This meant that if the sample of gabbro was poorly orientated between the antennae then it appeared to exhibit high signal attenuation and could be incorrectly detected as the highly attenuative kimberlite.

A number of possible mechanisms were explored to determine the cause of the observed phenomenon. Signal reflection from the rock surface was shown to be similar for gabbro and kimberlite in section 4.3.2. No large difference in reflected signal from either rock type was observed with varying rock orientation. It was therefore concluded that excessive signal reflection from the rock surface was not causing the observed phenomenon.

Signal diffraction and scattering through samples of gabbro were considered as possible causes for the apparent position dependent attenuation through gabbro. The occurrence of microwave signal diffraction through samples was demonstrated as shown below in figure 6.3.

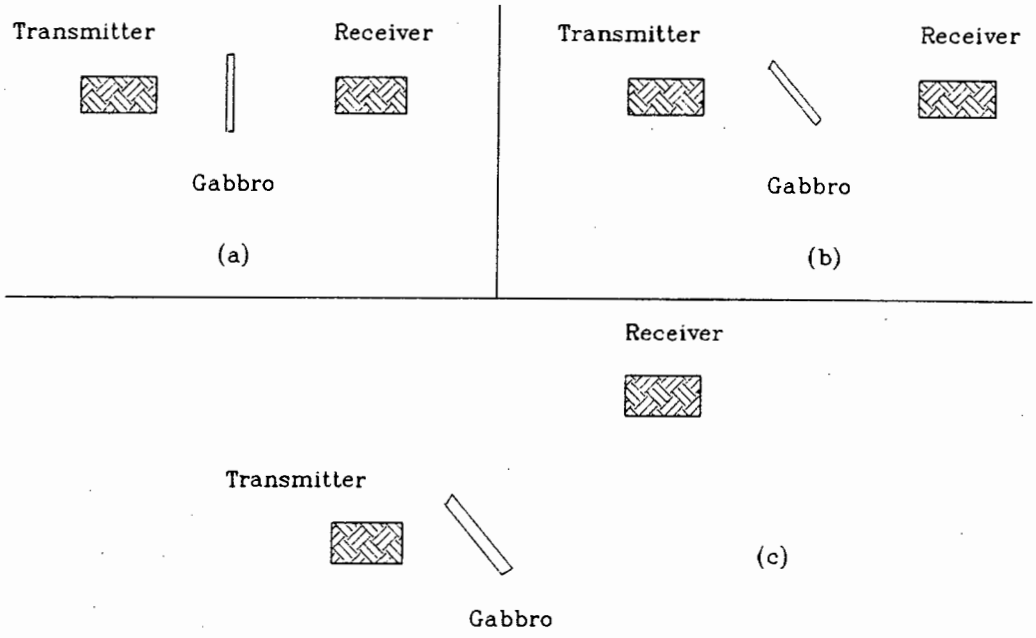

Fig. 6.3 Signal diffraction through gabbro.

When the units were correctly aligned as shown in figure 6.3a, with a flat sided gabbro sample placed perpendicular to the antennae, then low signal attenuation was recorded.When the sample was reorientated as shown in figure 6.3b then the attenuation due to the rock sample appeared to have increased. If the gabbro was left in this position and the receiver antenna was repositioned as shown in figure 6.3c then the original signal level was again observed. The rock was large enough to prevent any direct signal transmission between the antenna. This experiment indicated that the signal had been diffracted by the gabbro sample.

The antennae were left as positioned in figure 6.3c and randomly shaped samples of gabbro were examined. The results of this experimentation varied widely. The

received signal level could be improved by rocks that had faces that were close to flat. Some samples, however, demonstrated up to 26dB variation in received signal level due to orientation dependent signal scattering.

A few gabbro samples would reduce the received signal level, regardless of their orientation. These were the most irregular shaped samples of gabbro. This indicated that the microwave signal had been scattered by these rocks.The samples were chemically analysed to ensure that they had the same composition as other gabbro samples. It was found that with the antennae correctly aligned as shown in figure 6.3a, the level of signal attenuation was highest for rocks whose shapes deviated the most from flat sided.

Multiple signal reflections between the samples of gabbro and the antennae,resulting in standing waves, were also observed. Standing waves can arise from impedance discontinuities due to poorly matched detectors or antennae.An isolator acts as a well matched load and when connected as shown in figure 6.4,it will eliminate the effect of a poorly matched detector. A standing wave exists between the isolator and the detector due to the impedance discontinuity between them. The isolator prevents reflected signals from point B in figure 6.4 from reaching point A by absorbing the reflected signal.

The use of isolators at the transmitter and receiver eliminate the effect of standing waves between the antennae with no rocks placed between them.The impedance mismatch at the antenna\air interface could still establish a standing wave between the antennae but this effect was not observed.

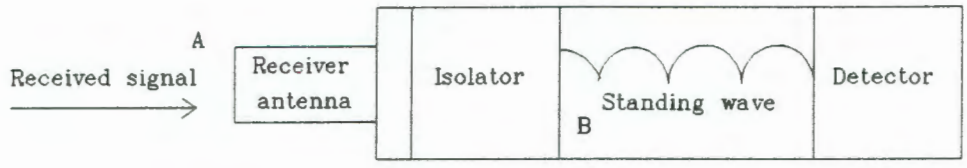

Fig.6.4 Elimination of detector impedance mismatch.

If the antennae were housed in metal containers that caused problems with reflected signals from their sidewalls then microwave absorbant foam could be fixed to the containers to eliminate this effect.The units shown in figure 6.5 have been covered with absorbant foam to eliminate this effect.

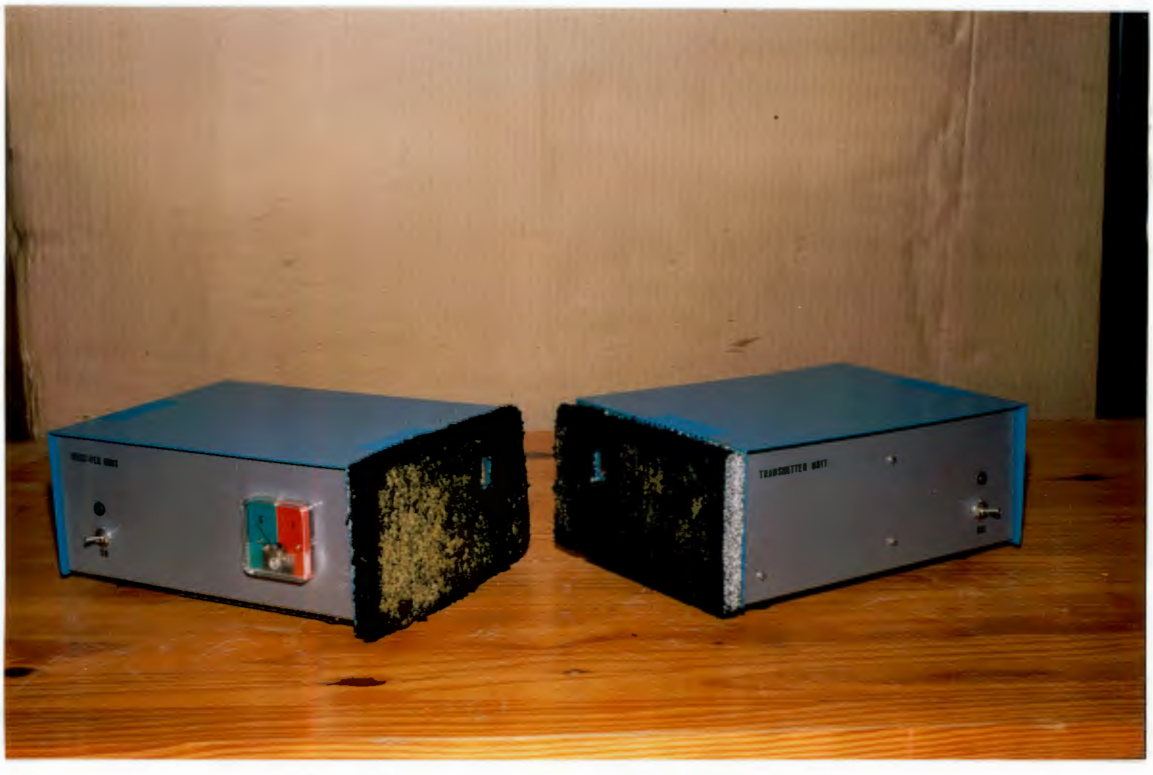

Fig.6.5 Elimination of sidewall reflections.

When a low loss material such as gabbro was placed between closely spaced antennae then the standing waves

were set up between the antennae and the material as shown in figure 6.6. This effect was observed as a periodic variation in signal amplitude as the position of the gabbro sample was varied between the antennae.

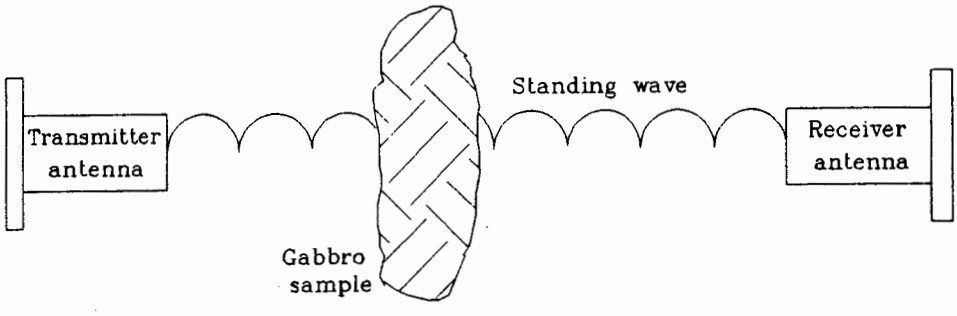

Fig.6.6 Standing wave due to rock sample.

The standing waves occurred as a result of addition or cancellation of reflected signals from the different surfaces of the rock. Although problems such as those discussed above were discovered by means of static experimentation, their importance could only be determined by means of dynamic experimentation.

6.1.2 Attenuation measurements through conveyor belt samples

Attenuation measurements were performed on conveyor belt samples to decide on a suitable conveyor belt for a laboratory test system as shown in figure 5.2. The ideal belt thickness is a radome thickness of $n\lambda/2$ where n = 1,2,3,4.... to allow for maximum signal transmission through the belt. Conveyor belt thickness of $n\lambda/4$ where n = 1,3,5,7... should be avoided as these allow minimum signal transmission through the belt.

The conveyor belt used should have as low a signal attenuation as possible to prevent it from adversely

affecting the system performance. A survey of 81 different conveyor belt samples was performed. These were made from rubber or plastic compounds with widely varying dielectric constant, ϵr, and it is important to use a belt with low loss to minimise signal attenuation through the belt sample. Some conveyor belts are steel reinforced and these belts had to be avoided because the microwave signal cannot be transmitted through the conductive steel layer.

The belt samples examined exhibited various levels of attenuation from 0.22dB to 15.5dB at 35GHz. The belt chosen had less that 2dB loss. Although the conveyor belt loss was constant and was calibrated out of the system it could have had an adverse effect on the dynamic range of the system if it was too high (eg.15dB).

6.2 Dynamic Results

An experimental laboratory scale conveyor belt capable of moving at a speed of 5m/s was provided by De Beers. 5m/s is the conveyor belt velocity commonly used in high throughput automatic sorting machines. The microwave transmit and receive antennae were mounted above and below the conveyor belt as indicated in figure 5.2. The low loss conveyor belt was channelised to ensure that the rock samples passed directly between the antennae.

The pre-production model microwave receiver with the 0-5 Vdc output was used for these experiments. The 0-5Vdc output was linked to a personal computer via an A/D convertor. The received signal level was recorded as the rocks were passed between the antennae. Repeated tests were performed with many different samples of gabbro and kimberlite. This work was performed in conjunction with De Beers personnel at De Beers Diamond Research Laboratories.

The data shown in figure 6.8 indicates the frequency distribution of received signal level through samples of gabbro and kimberlite. This data was obtained from 5640 tests on the rock samples.

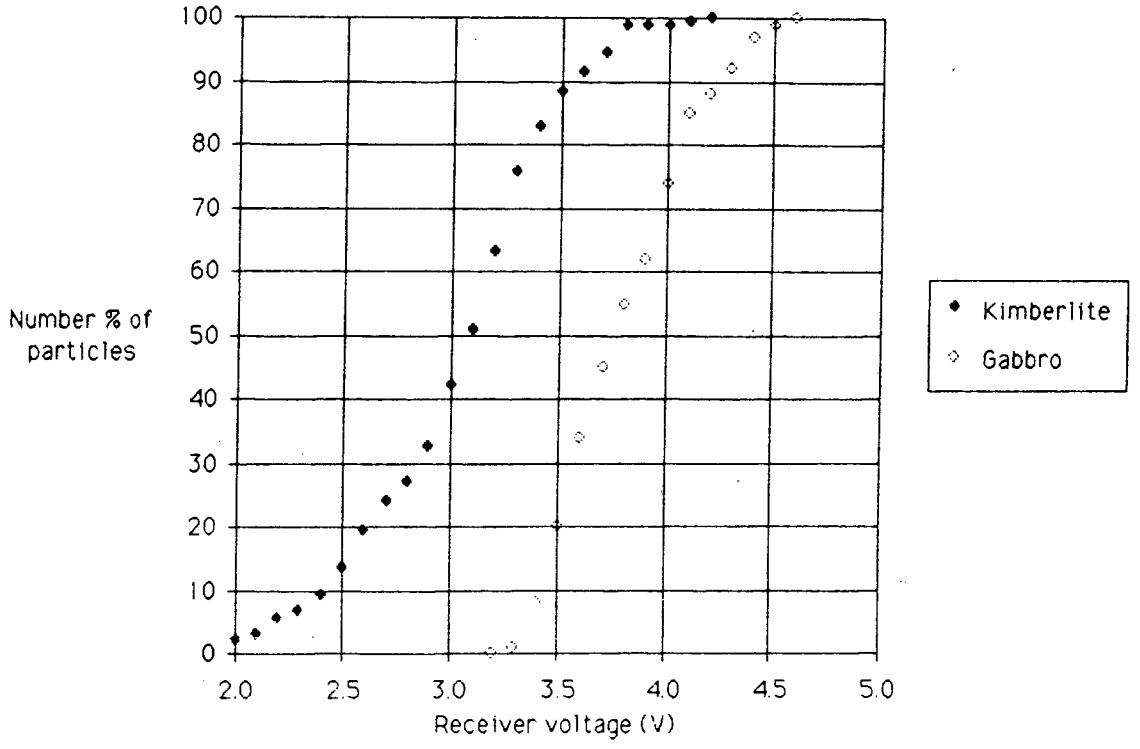

Fig.6.7 Cumulative transmitted power number frequency distribution.

The coefficients of variation for gabbro and kimberlite samples were examined. Fourty replications on 146 different rock samples were performed to obtain the data shown in figure 6.8. These data indicate the distribution of the coefficients of variation for each set of 40 replicates.

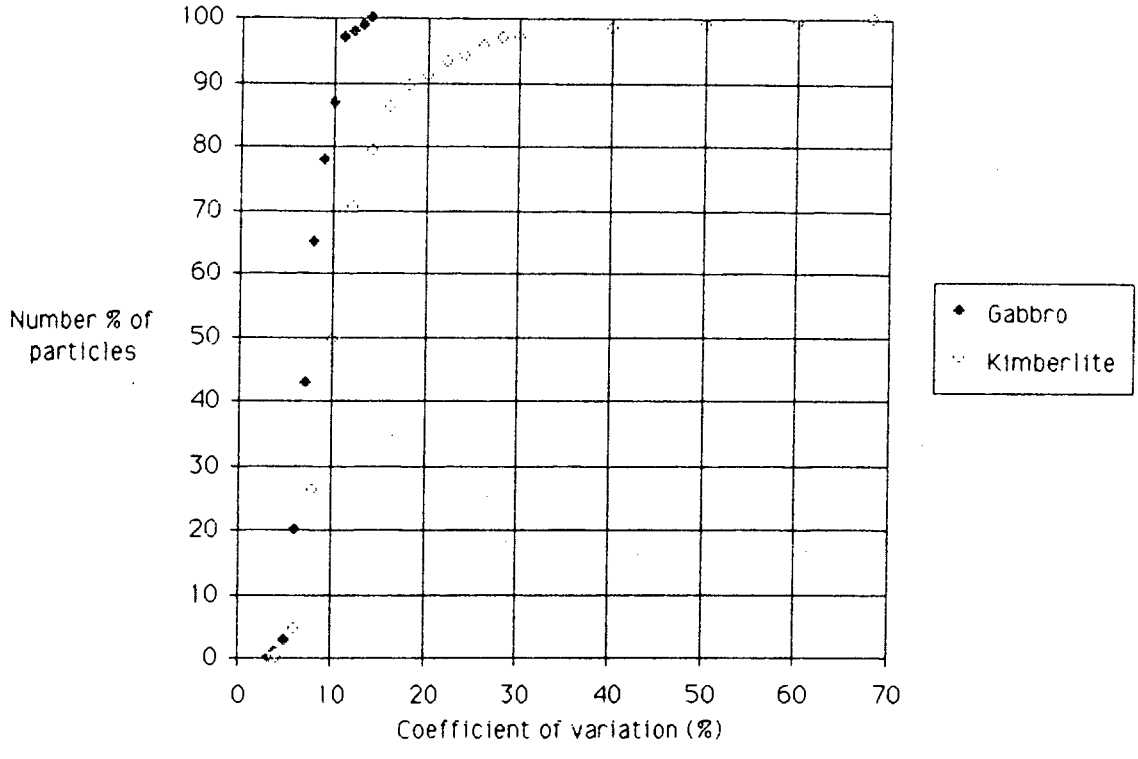

Fig. 6.8 Distribution of coefficients of variation.

It can be seen from figure 6.8 that the gabbro samples displayed a 10% variation in signal level whilst the coefficient of variation for kimberlite was much greater. This was due to the inhomogenous composition of kimberlite which results in anisotropy of dielectric constant through this rock type.The size and shape of the samples were also influencial factors.

The data displayed in figure 6.9 represent the percentage of

correctly identified kimberlite versus the percentage of correctly identified gabbro rejected. These data were obtained from 5640 tests on rock samples. It can be seen from figure 6.9 that a trade off is possible between the percentage of retained kimberlite and the percentage of rejected gabbro. The highest percentage of kimberlite is retained when the lowest percentage of gabbro is rejected. Figure 6.9 indicates that with a 93% retention of kimberlite, 67% of the waste gabbro can be rejected.

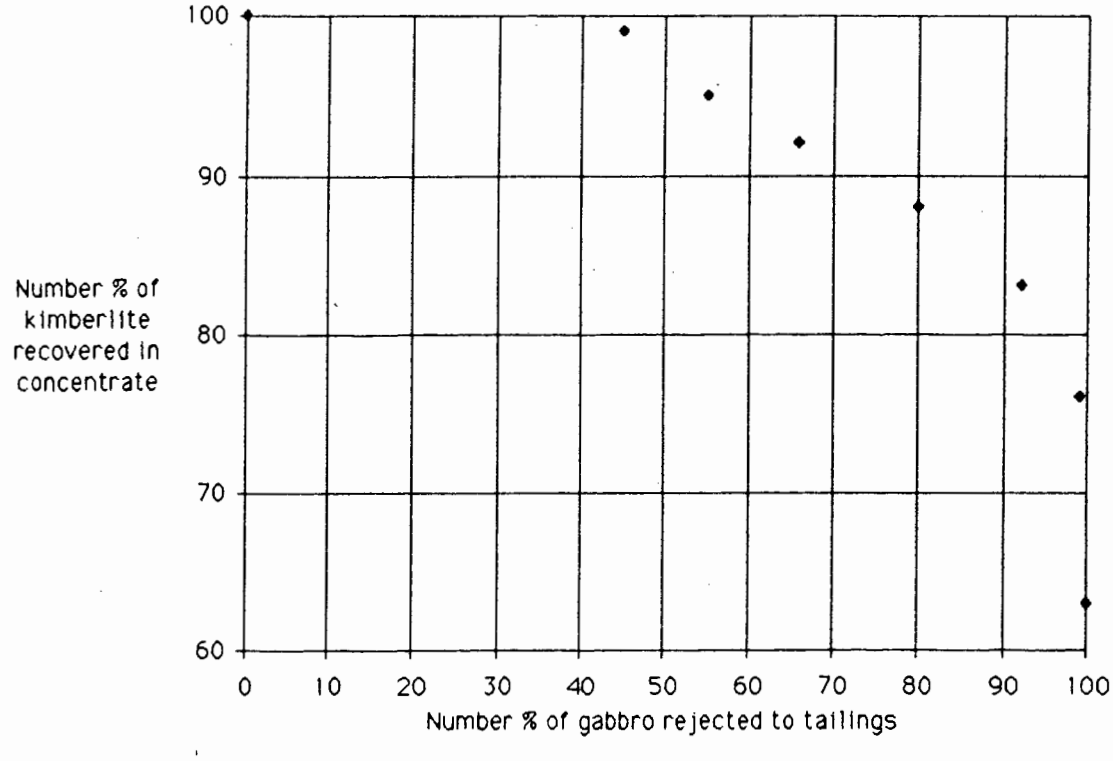

Fig. 6.9 Gabbro rejection curve.

It was noted that the rejection of gabbro was dependent on the shape of the sample. The scattering of microwave signal by some gabbro samples led to their misidentification as kimberlite. The size variation of rocks was also found to be a critical factor in the identification of rock samples. Thin kimberlite samples were occasionally misidentified as gabbro due to the low signal attenuation through the thin slice.

The results shown in this section indicate that a high percentage of gabbro can be correctly identified using this equipment. This work has resulted in the filing of two provisional patent applications ,which are currently not open for public inspection.

7.1 Future Research

The existing microwave equipment functions well as a rock by rock discrimination device for the recognition of gabbro and kimberlite. It may, however, be possible to improve the system performance by either rejecting more of the gabbro and/or retaining more of the kimberlite.

The use of an optical technique for sizing of rock samples should yield improved results when signal attenuation is related to sample size. This would result in the correct detection of some of the thin and therefore less attenuative kimberlite samples. The combined use of microwave and gamma ray measurements as mentioned in [8] may also result in improved gabbro rejection. Gabbro and kimberlite have,in general, different densities, as mentioned in section 1, and gamma ray measurements give an indication of sample density. The effect of combining these measurements may well result in improved gabbro rejection.

Standing waves were observed between some gabbro samples and the antennae. The use of a swept frequency technique using, for example, wideband varactor tuned Gunn oscillators, may help to reduce the adverse effect of these standing waves by averaging the observed attenuation over the swept frequency range. Figure 7.1 indicates the effect of sweeping frequency on the standing wave pattern between the antennae.

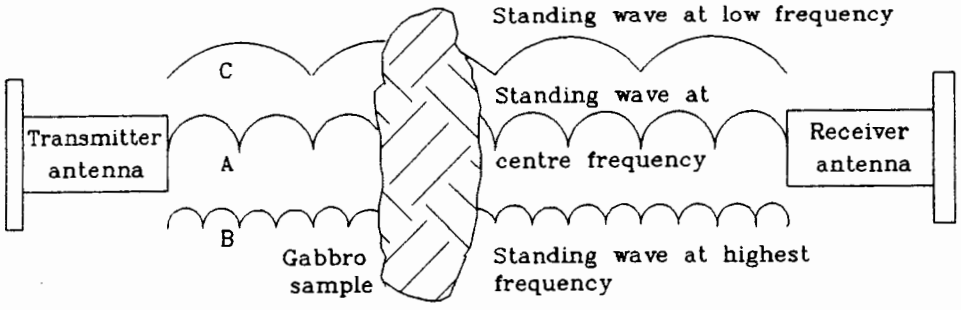

Fig.7.1 Effect of sweeping frequency.

The standing wave pattern,A,represents the position of nulls and peaks at the centre frequency.The effect of increasing frequency is shown by pattern B whilst pattern C demonstrates the effect of decreasing frequency.By sweeping frequency it would be possible to obtain an indication of the average attenuation through a rock sample. Note that this technique is complicated by many factors such as oscillator output power variation over the swept frequency range and is not easily implemented in practise.

If improved results are required then consideration could be given to the use of microwave phase shift measurements through rock samples. This technique has already been the subject of two provisional patent applications. These are,however,not open for public inspection. Capacitance measurements performed at frequencies up to 50MHz indicate that kimberlite has a consistently higher ϵ_r than gabbro. Kimberlite should exhibit a larger propagation delay or signal phase shift than gabbro and microwave signal phase shift could be used to differentiate between them. The combined use of signal attenuation and phase shift could be considered.

The use of phase shift measurements may significantly reduce the problem of rejecting oddly shaped gabbro samples because these measurements are less dependent on the received signal amplitude. It should be noted that the development time of an accurate microwave phase shift meter is long due to its inherent complexity.

Microwave attenuation and phase shift measurements may be suitable for application in other areas of rock sorting.However, with highly attenuative substances it may be necessary to reduce the operating frequency to ensure that the overall attenuation is not too high. This would result in increased antenna aperture area due to the lower frequencies, limiting the process to the sorting of larger samples than at higher frequencies.

This problem could be overcome by using reduced aperture antennae. It is possible to dielectrically load an antenna to reduce its aperture area. A reduced aperture dielectrically loaded square waveguide antenna is illustrated in figure 7.2.

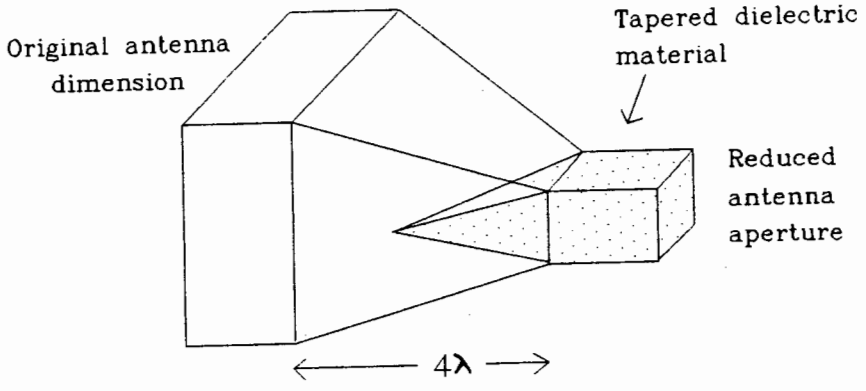

Fig. 7.2 Dielectrically loaded antenna.

The dimensions of the antenna's output aperture are influenced

by the dielectric constant of the chosen dielectric material. The antenna aperture of the dielectrically loaded antenna will be $l = l/\sqrt{\epsilon_r}$. Thus if a dielectric material with $\epsilon_r=4$ were used then the antenna aperture area would be reduced to 1/2 of it's original dimension. The dielectric material is tapered to allow a smooth transition from the initial dimensions to the reduced dimensions.

A different form of reduced aperture antenna that could be experimented with in this application is a microstrip resonant patch antenna. These antennae can be fabricated to give an X band antenna with similar aperture dimensions to the 35GHz antennae described in section 4.1.1, if a high dielectric microstrip material, such as RT DUROID 6010 ($\epsilon_r=10$) is used.

It is clear that there are many potential applications for microwave measurements in ore sorting but more research is required before these become practical.

7.2 Conclusions

Microwave equipment was constructed and tested to differentiate between samples of gabbro and kimberlite on a rock by rock basis.

A microwave rock heating scheme to differentiate between kimberlite and waste rock was investigated. It was found that the impracticability of building a 7MW microwave power plant for heating the required tonnage of rock was too great for such a system to be viable in this application.

Low power microwave transmission through rock samples were examined. Microwave phase shift measurements were not considered due the the very high cost, complexity and the long development time of such a system and the immediate requirement of a solution to the waste rock problem at Premier Mine. The use of reflected microwave signals from rock samples was found to be an unreliable means of rock differentiation due to the similar levels of reflected signal from the different rock types.

Microwave signal attenuation through rock samples was investigated. It was found that there was a detectable difference in signal attenuation through kimberlite and the waste rocks gabbro and felsite. The difference in microwave signal attenuation between kimberlite and gabbro was found to increase with increasing frequency.

A means of applying microwave signal attenuation measurements to rock samples had to be chosen. It was found that the use of microwave signal transmission through overmoded waveguide structures was not a viable method to obtain attenuation measurements in this application due to the low energy density in these waveguides.

Microwave signal transmission between two antennae was found to be a viable technique to obtain attenuation measurements through rock samples. Equipment was designed and constructed to perform attenuation measurements on rock samples. A range of operating frequencies were examined. An operating frequency of 35GHz was chosen due to the small antenna aperture area at this frequency and the fact that a large attenuation difference existed between kimberlite and the waste rock at this frequency.

Static tests with different rock samples and the abovementioned equipment revealed problems such as signal diffraction and scattering through the low loss gabbro. Multiple reflections were observed between samples of gabbro and the antenna. The shape of the gabbro sample influenced the magnitude of these phenomenon. The significance of these observed problems could not be gauged without performing dynamic tests.

Dynamic tests on many different rock samples were performed using a laboratory test system with a conveyor belt moving at a speed of 5m/s. It was found that 93% of the kimberlite could be correctly detected whilst rejecting 67% of the gabbro. This meant that a viable, working system has been developed. This work has led to the filing of the patents mentioned in section 6.2.

LIST OF REFERENCES

[1] "General information for visitors to Premier Mine". De Beers Consolidated Mines Limited. Premier Mine Division.

[2] M.A. STUCHLY, "Fundementals of the interaction of radio-frequency and microwave energies with matter", Radiation Protection Bureau, Health and Welfare Canada, Ottawa, Ontario K1A 0l2.

[3] Electrical Properties of Rocks, E.I. PARKHOMENKO, PLENUM PRESS, NEW YORK, 1967.

[4] A. KLEIN, "Microwave determination of Moisture in Coal - A comparison of attenuation and phase measurement", 10th European Microwave Conference 1980, pp 526 - 530.

[5] A. KLEIN, "Microwave determination of moisture in coal: Comparison of attenuation and phase measurements", Journal of Microwave Power VOL 16 (1981) pp 289 - 304.

[6] A. KLEIN, "Microwave determination of moisture compared with Capacitive, Infrared and Conductive measurement methods. Comparison of on line measurements at coal preparation plants", European Microwave conf. Proc. 14th, 1984, pp 661 - 666.

[7] A. KLEIN, "Comparison of rapid moisture meters", Aufbereitungs Technik No1/1987, pp 10 - 16.

[8] C.B. ZEHNDER, "Application of the Combination Microwave - Gamma ray gauge to wood chip weight and moisture measurement", Pulp and paper magazine of Canada,1967, VOL. 10, pp T678 - 688.

[9] T.T. CHEN, J.E. DUTRIZAC, K.E. HAQUE, W.WYSLOUSIL, S. KASHYAP; "The relative Transparency of Minerals to Microwave Irradiation," Canadian Metallurgical Quarterly, VOL. 23, No. 3, pp349 - 351, 1984.

[10] G.E. FANSLOW, D.D. BLUHM, S.O. NELSON, "Dielectric heating of Mixtures Containing Coal and Pyrite," Journal of Microwave Power, 15 (3), 1980, pp 187 - 191.

[11] Principles of Active Network Synthesis and Design, Gobind Daryanani, John Wiley and Sons, New York, 1976.

[12] M.A. ALDERA, A 10GHz Rock Differentiation System, Undergraduate thesis project, UCT, 1986.

BIBLIOGRAPHY

Brooks, R.0. Laboratory Manual for Microwave Measurements Prentice Hall inc, Englewood Cliffs, New Jersey.

Horowitz, P and Hill, W. The Art of Electronics Cambridge University Press, Cambridge, 1984.

Huxley, L.G.H. A survey of the principles and practice of waveguides, Cambridge University Press, 1947.

King, R.J. Microwave homodyne systems Peter Peregrinus Ltd.

Liao, S.Y. Microwave Devices and Circuits Prentice Hall 1980, Englewood Cliffs, New Jersey.

Precision Microwave and RF test equipment: Narda Microwave Corporation, Plainview, New York.

Silver, S. Microwave Antenna theory and design McGraw-Hill Book Company, INC. 1949.

Sucher, M and Fox, J. Handbook of Microwave Measurements VOL 11. Polytechnic Press, a division of J. WILEY + SONS. INC.

APPENDIX A

AN APPROXIMATE CALCULATION OF THE POWER REQUIREMENTS OF AN ON LINE MICROWAVE ROCK HEATING PLANT.

This calculation is based on the work of M.A.Aldera [12]. It was found by experimentation that the temperature of a 230g kimberlite sample was raised by 50°C after a one minute exposure to an incident power of 500W at a frequency of 2.45 GHz.

From elementary Physics:

$$\Delta H = mc\Delta T$$

where ΔH = the change in the samples heat content in Joules.
m = the mass of the samples in grams
c = the specific heat capacity of the sample

Now if t is the time period of heating then

$$\Delta H/\Delta t[\text{Watts}] = mc\Delta T/\Delta t$$

where $\Delta H/\Delta t$ = the power required in Watts to heat the sample by a given temperature ΔT in a given time.
The specific heat capacity "c" lies within the range 0 to 1. A value of c = 0.5 is assumed for this calculation.

The power required to heat a 230g kimberlite sample by 50°C in 1 minute is therefore:

$$P_i = \Delta H/\Delta t = 230 * 0.5 * 50/60 = 95.8W$$

A transmission line equivalent circuit of the rock heating process is indicated in figure A1.1.

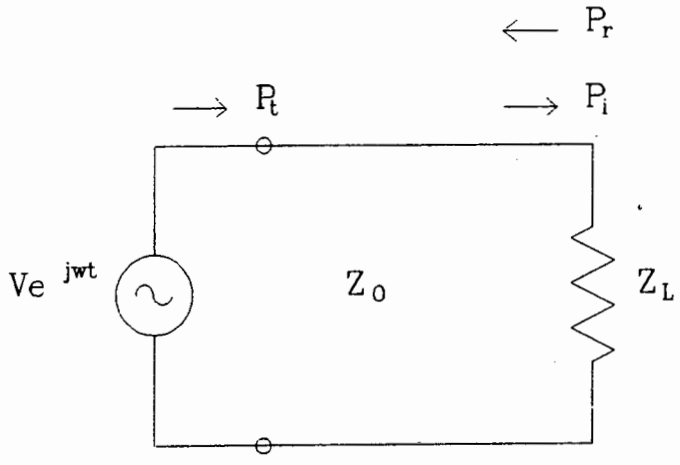

Key

P_t =500 Watts

P_i =95.8 Watts

P_r =Reflected power

Z_L=Load impedance

Z_0=Characteristic impedance of the line.

Fig A1.1 Transmission Line Equivalent Circuit

Since $Z_1 \neq Z_o$, a certain amount of signal reflection takes place at the rock / air interface. The power absorbed by the rock, P_i, is given by

$$P_i = (1 - |\rho|^2)P_t$$ where ρ is the reflection coefficient of the rock.

Substituting known values of P_i and P_t we find

$$1 - |\rho|^2 = 0.19$$

indicating that 19% of the transmitted power is absorbed in the rock (Z_1) whilst 81% of the transmitted power is reflected.

If rocks are transported on a conveyor belt at a rate of x tons/second and the required change in the temperature of kimberlite is T_k[°C] then

$$P_i = (1- |\rho|^2)P_t = m_k c_k \Delta T_k / \Delta t$$

therefore

$$P_t = 0.5 * \Delta T_k * 10^6 / [1- |\rho|^2]$$

Assuming that the rocks are transported at a rate of 15 tons/minute, (0.25 tons / second) and the required rise in the temperature of kimberlite is 10°C to effect reliable rock differentiation then

$$P_t = 0.5 * 0.25 * 10^7 / 0.19$$
$$= 6.58MW$$
$$= \text{required microwave power}$$

This calculation may yield a pessimistic result due to the approximate nature of the data used but serves to indicate that an excessive amount of microwave power would be required to raise the temperature of the desired tonnage of ore by a mere 10°C.

APPENDIX B: Design criteria for square waveguide antennae and rectangular to square waveguide transformers

All dimensions in mm.

	A	B	C	D	X	L	Hole diameter
X band	16.3	15.5	41.3	20.6	22.9	50.8	4.3
J band	12.1	12.6	33.3	16.7	15.8	50.8	4.7
K band	8.1	8.5	22.2	11.1	10.7	50.8	2.9
Q band	6.4	6.7	19.1	9.5	7.1	50.8	3.0

Square waveguide antennae.

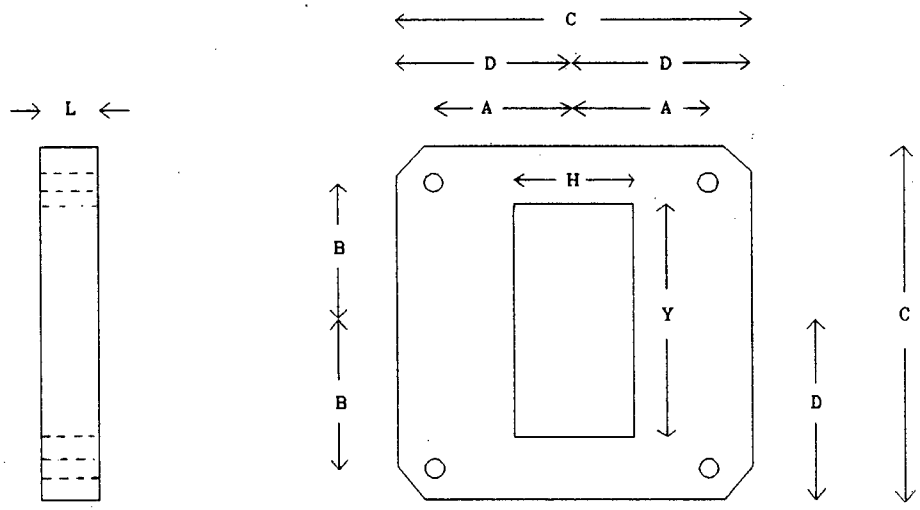

	A	B	C	D	L	H	Y	Hole diameter
X band	16.3	15.5	41.3	20.6	9.9	15.2	22.9	4.3
J band	12.1	12.6	33.3	16.7	6.3	11.2	15.8	3.7
Q band	6.4	6.7	19.1	9.5	2.7	5.0	7.1	3.0

All dimensions in mm.

Rectangular to square waveguide transformers

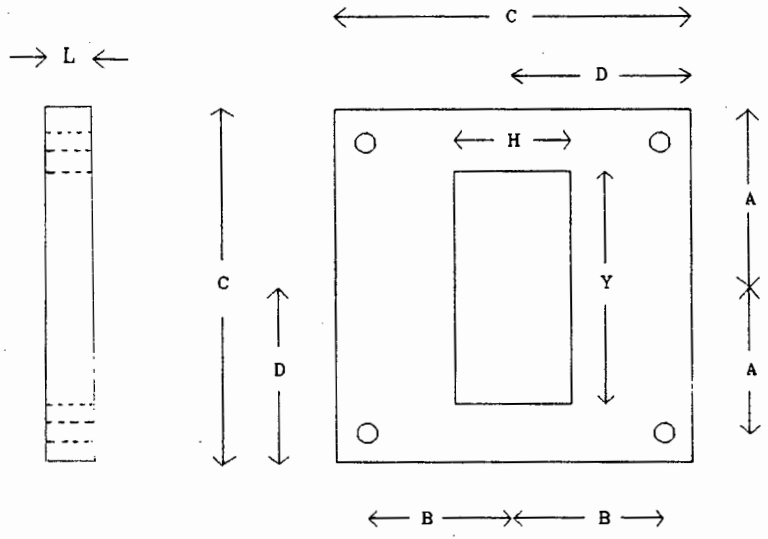

All dimensions in mm.

	A	B	C	D	L	H	Y	Hole diameter
K band	8.1	8.5	22.2	11.1	4.1	6.8	10.7	2.9

Rectangular to square waveguide transformer

APPENDIX C: Printed Circuit Board foil patterns.

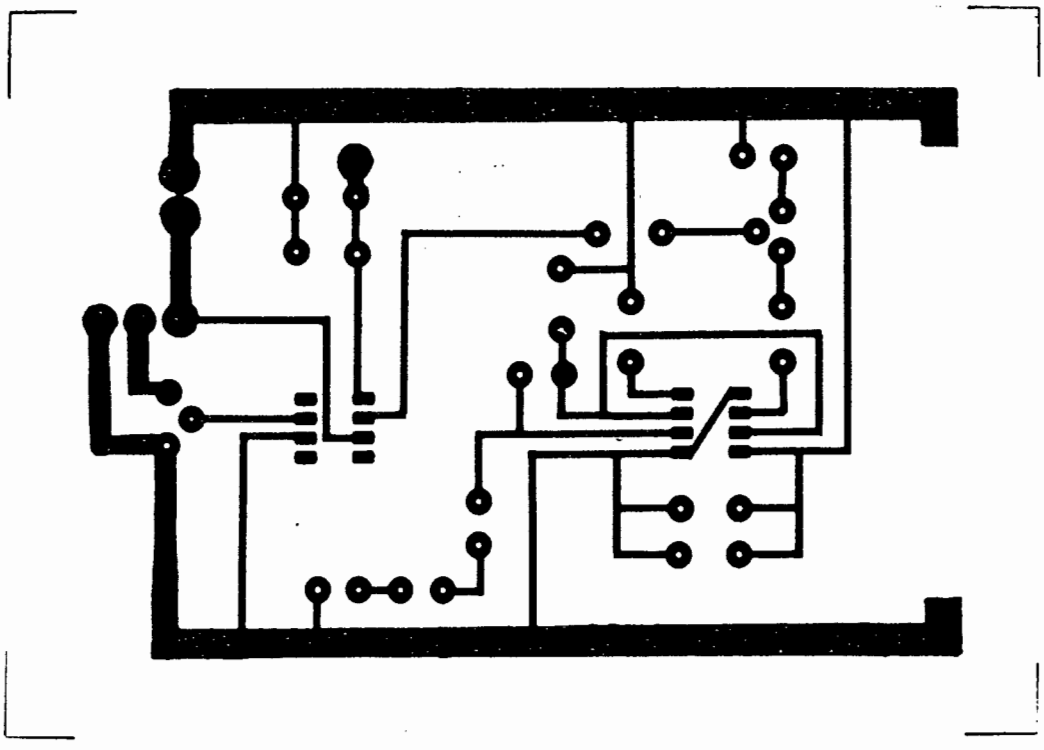

Transmitter printed circuit board foil pattern.

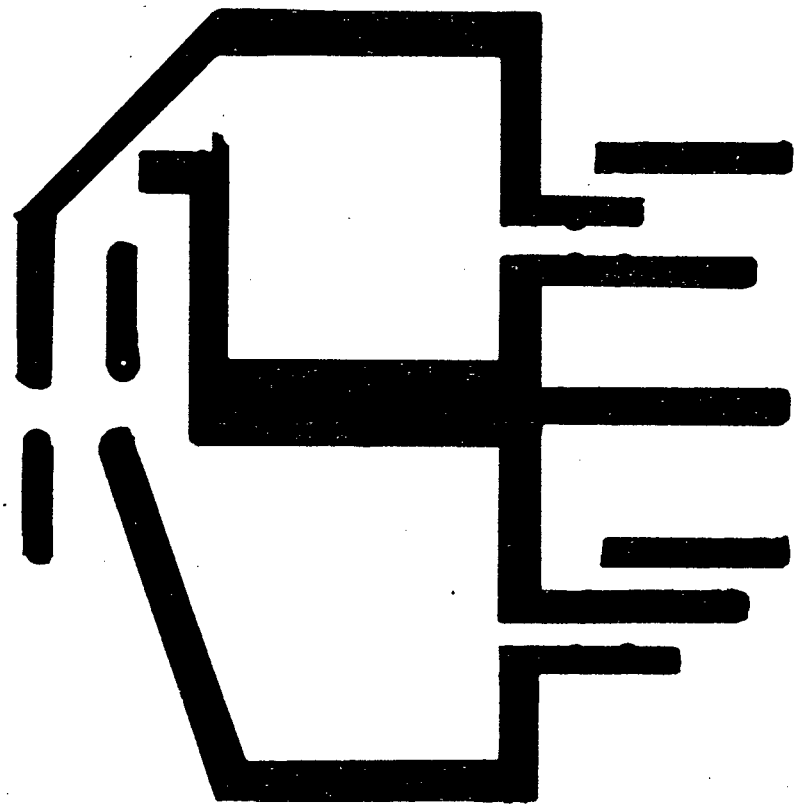

Transmitter power supply printed circuit board foil pattern.

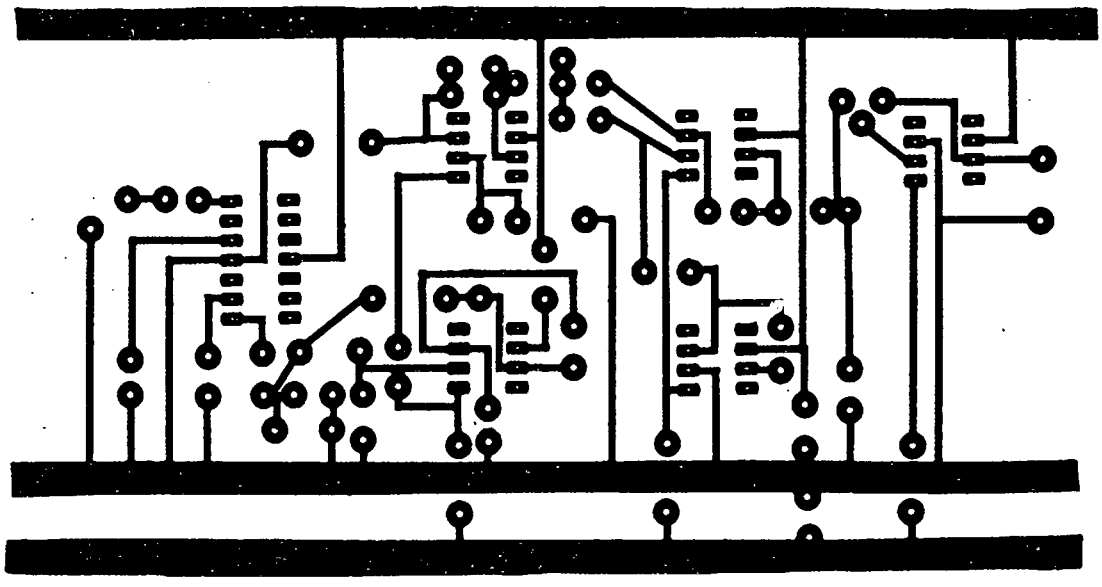

Receiver printed board foil pattern.

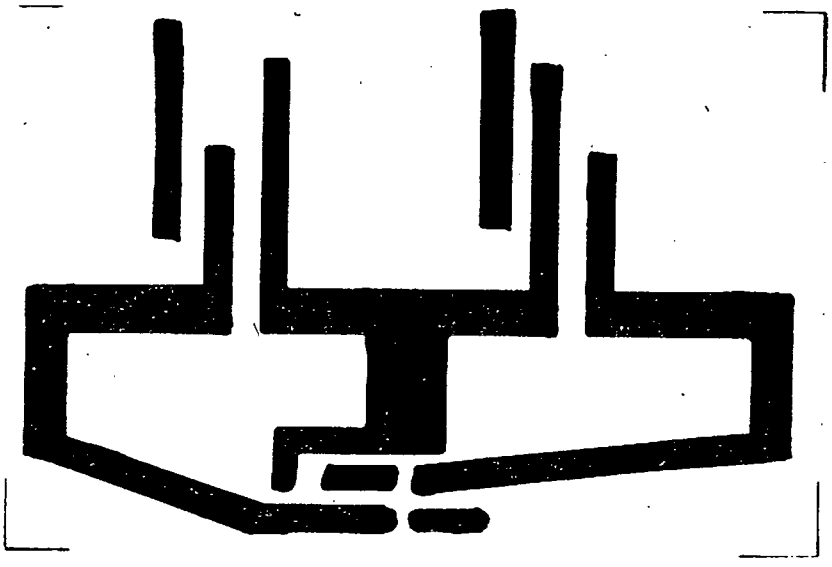

Receiver power supply printed circuit board foil pattern.